NASA CR-122350

INSTRUMENTATION FOR RADIO ASTRONOMY MEASUREMENTS ABOARD THE IMP-I (EYE) SPACECRAFT

Fred T. Haddock
Radio Astronomy Observatory
2235 Space Research Building
University of Michigan
Ann Arbor, Michigan 48105

June 1971

Final Engineering Report for Period May 1969 - March 1971

Prepared for

GODDARD SPACE FLIGHT CENTER
Greenbelt, Maryland 20771

(NASA-CR-122350) INSTRUMENTATION FOR RADIO ASTRONOMY MEASUREMENTS ABOARD THE IMP-I SPACECRAFT Final Engineering Report, May 1969 - Mar. 1971 F.T. Haddock (Michigan Univ.) 1 Jun. 1971 80 p CSCL 03A G3/30

N72-18838

Unclas
17807

TECHNICAL REPORT STANDARD TITLE PAGE

1. Report No.	2. Government Accession No.	3. Recipient's Catalog No.
UM/RAO 71-5		
4. Title and Subtitle INSTRUMENTATION FOR RADIO ASTRONOMY MEASUREMENTS ABOARD THE IMP-I (EYE) SPACECRAFT		5. Report Date June 1, 1971 6. Performing Organization Code
7. Author(s) Fred T. Haddock		8. Performing Organization Report No.
9. Performing Organization Name and Address University of Michigan 2235 NASA Space Research Building Ann Arbor, Michigan 48105		10. Work Unit No. 11. Contract or Grant No. NAS5-11174
12. Sponsoring Agency Name and Address Goddard Space Flight Center Greenbelt, Maryland 20771		13. Type of Report and Period Covered Final Engineering May 1969 - March 1971 14. Sponsoring Agency Code

15. Supplementary Notes

Final Engineering Report. Scientific aspects and results will be published separately.

16. Abstract

Describes the design considerations and performance parameters of a satellite-borne instrumentation system designed and constructed at the University of Michigan Radio Astronomy Observatory. The system is designed to make radio astronomy measurements at eight discrete frequencies from 50 kHz to 3.53 MHz. These measurements are to detect Solar and Jovian radio frequency bursts and to determine the average cosmic background radiation level down to 50 kHz.

Procedures used for preflight and inflight calibration of the radiometer are discussed. A description of the ground support equipment used for preflight testing is given.

17. Key Words (Selected by Author(s))	18. Distribution Statement
IMP-I Spacecraft. Low frequency radio astronomy measurements. Solar and Jovian radio frequency bursts. Cosmic background radiation.	

19. Security Classif. (of this report)	20. Security Classif. (of this page)	21. No. of Pages	22. Price*
UNCLASSIFIED	UNCLASSIFIED	80	

PRECEDING PAGE BLANK NOT FILMED

PREFACE

This is the final technical report concerning the instrumentation designed and constructed at the University of Michigan Radio Astronomy Observatory Laboratory for making satellite-borne radio astronomy observations at eight discrete frequencies from 50 kHz to 3.53 MHz.

The purpose of the observations is threefold: to measure the average level of galactic radio emission, to detect Solar radio frequency bursts, and to detect radio frequency emission from Jupiter.

Procedures used for preflight and inflight calibrations of the radiometer are discussed. A description of the ground support equipment used for preflight testing is given.

The instrument was successfully launched aboard the IMP-I (1971 019A) spacecraft on 13 March, 1971 into an elliptical orbit having the following approximate parameters: perigee, 242 kilometers; apogee, 206,000 kilometers; inclination to the equator, 29°; period, 101 hours. The spacecraft is spin-stabilized with the spin axis approximately 90° to the ecliptic plane and has a spin rate of approximately 5.6 revolutions per minute.

The initial data from the experiment looks excellent and the instrument should successfully fulfill its designed mission.

The scientific aspects and results of this program will be published separately.

TABLE OF CONTENTS

PAGE

LIST OF FIGURES

INSTRUMENTATION FOR RADIO ASTRONOMY MEASUREMENTS ABOARD THE IMP-I SPACECRAFT

I. INTRODUCTION

This report describes the design considerations and performance characteristics of an instrumentation system designed and constructed at the University of Michigan Radio Astronomy Observatory Laboratory for satellite-borne radio astronomy observations. These observations are carried out at eight discrete frequencies from 50 kHz to 3.53 MHz (50, 80, 130, 230, 350, 600, 900 and 3530 kHz), and their purpose is to detect Solar and Jovian radio frequency bursts, and to measure the average level of cosmic background radiation down to 50 kHz. Due to the wide frequency range covered by the radiometer, it not only provides correlation with the data obtained from our earlier radiometers flown on OGO spacecrafts I-V, but also extends our observations down to lower frequencies. A similar experiment was flown on the OGO-V spacecraft but, due to a high level of RFI on the spacecraft, little useful data was obtained at the lower frequencies.

The radiometer system, as shown in Figure 1, consists of a dipole with a half-length up to 180 feet, a pair of preamplifiers located at the antennas, a stepping superheterodyne receiver, a noise calibrator, and a power supply. The antenna assemblies and preamplifiers were furnished by Goddard Space Flight Center (GSFC).

The antennas are of the motor-driven type which may be extended or retracted to any length, up to a maximum length of 180 feet, upon ground command. There are telemetry outputs which indicate the length of the antenna elements during deployment.

The first stage in the receiver consists of a matched pair of low-noise broadband preamplifiers, each having an unbalanced input and output, and one of which shifts the phase of the incoming signal by 180 degrees. The preamplifier inputs are filtered to prevent telemetry signals from entering the radiometer. The antenna and preamplifier input circuits are untuned.

Following the preamplifiers is an RF summing amplifier. A low pass filter in the summing amplifier rejects undesired signals above 3.53 MHz.

Following the summing amplifier is a balanced diode mixer which is fed from a complex of eight crystal-controlled oscillators. The selection of the active oscillator is controlled by internal logic which is synchronized with the spacecraft data system. Sequencing the oscillator selection achieves the tuning in eight steps across the signal passband of the receiver with center frequencies from 50 kHz to 3.53 MHz. The mixer feeds a 10.7 MHz crystal filter which determines the overall system bandwidth of 10 kHz (6 db). A telemetry output is provided to identify the operating center frequency of the radiometer.

After suitable buffering, the output of the crystal filter is fed to a four stage, gain-controlled (AGC) IF amplifier. The response of this amplifier is logarithmic and has a useful dynamic range of 55 db. Following the IF amplifier is an envelope detector, the bias of which is temperature stabilized. This bias voltage is fed to the telemetry system for monitoring purposes. The output of the detector feeds an emitter follower stage which provides the AGC voltage for the IF amplifier and isolates the detector from the final signal conditioning circuitry.

The final conditioning of the radiometer data consists of establishing the post-detection time constant of 0.12 seconds and constraining the DC output voltage to a range of 0.0 to 5.1 volts. This final stage constrains the voltage range and provides a low output impedance to achieve compliance with the spacecraft telemetry system requirements. This DC voltage is the radiometer output.

A solid-state noise diode and an associated amplifier are incorporated in the radiometer for inflight calibration. The noise calibrator provides a white noise source over the operating frequency of the radiometer. Four levels of calibration are provided through the use of a logic-controlled attenuator. The sequencing of this attenuator is synchronized with the spacecraft telemetry system. Calibration occurs every 2.91 hours and requires 81.92 seconds. Alternate preamplifiers are calibrated each calibration cycle. Telemetry outputs are provided which indicate the fact that a calibration cycle is occurring, which preamplifier is being calibrated during that cycle, the calibration levels, the current through the noise diode, and the temperature of the noise diode.

A voltage regulator circuit was included in the system to isolate the radiometer from noise associated with the spacecraft power supply and to insure stable voltages for critical circuits in the radiometer. Current limiting was incorporated to protect the series regulating element from accidental or transient shorts. Extensive filtering was provided to reduce conduction of RFI from the regulator circuitry to critical RF circuits. A telemetry output is provided to monitor the regulator output voltage.

The radiometer has two modes of operation: a frequency stepping mode and a single frequency mode. The frequency stepping mode is controlled, as mentioned earlier, by internal logic triggered by a timing signal from the spacecraft.

The change from this mode of operation to the single frequency mode is controlled by a ground command. The desired operating frequency may also be selected by ground command once the radiometer has been placed in the single frequency operating mode. A third ground command provides the dual function of turning the radiometer on and/or placing the radiometer in the frequency stepping mode.

An internal free-running multivibrator provides the radiometer timing signal in the event the spacecraft timing signal is lost. The frequency of this multivibrator is adjusted such that useful radiometer data may be obtained even though the frequency stepping is no longer synchronized with the data system.

A brief description of the ground commands used by the radiometer is given below:

1. Power ON/Enable Frequency Stepping (54P, 60T) - These two cross-strapped commands provide the dual function of turning the radiometer on and/or placing the radiometer in the automatic frequency stepping mode as described above.

2. Disable Frequency Stepping (63T) - This command places the radiometer in the single frequency mode of operation.

3. Single Frequency Step (62T) - The operating frequency of the radiometer is changed by one step (eg. 50 to 80 kHz) each time this command is sent.

4. Power OFF (61T) - Self explanatory.

II. DETAILED DESCRIPTION OF INSTRUMENT

A. ANTENNA ASSEMBLY

1. General Operation

The antenna system used by the UM/RAO experiment consists of a dipole pair mounted in the X axis of the IMP-I spacecraft. The antennas have a nominal dipole half-length of 150 feet when erected, with a maximum erection length of 180 feet. The antennas are motor-driven and may be individually erected or retracted by ground command. Length sensors are associated with each element and telemetry outputs are provided to monitor the extended element length.

The antenna element is fabricated from beryllium copper with the inboard 125 feet of the element coated with Dupont Kapton. The element is heat treated in such a manner that in the relaxed state it forms a cylindrical tube approximately 0.50 inches in diameter.

A detailed description of the antenna assembly will not be given in this report as the antennas were furnished as part of the IMP-I spacecraft.

2. Antenna Equivalent Circuit

The equivalent circuit for the dipole antenna is shown in Figure 2. The approximate free space values for R_A and C_A may be calculated from:

$$R_A = 80\,\pi^2\,(h/\lambda)^2 \qquad (1)$$

and

$$C_A = \pi\,\epsilon_o h/\{\ln(h/a) - 1 - 0.5\ln\,(2h/\lambda)\} \qquad (2)$$

where:

R_A = Antenna radiation resistance

C_A = Antenna capacitance

h = Dipole half-length

λ = Free space wavelength

ϵ_o = Free space permittivity (8.85×10^{-12} farads/meter)

a = Antenna wire radius (0.25 inches)

Using equation (1) to calculate the radiation resistance for an 80 foot dipole, it is possible to predict values ranging from 1.31×10^{-2} ohms at 50 kHz to 65.0 ohms at 3.53 MHz.

Using equation (2) to calculate the antenna capacitance for the same length dipole, it is possible to predict values ranging from 70 picofarads at 50 kHz to 90 picofarads at 3.53 MHz.

The use of both of these equations assumes the dipole acts as an electrically short antenna at these frequencies. This is not strictly accurate but the values obtained are accurate within a few percent.

C_B in the antenna equivalent circuit is stray capacitance. This stray capacitance is due to the proximity of grounded surfaces to the antenna and signal leads. Careful measurements were made of this capacitance with the antennas mounted in the spacecraft and showed an equivalent capacitance of approximately 42 picofarads. The cables between the antenna and preamplifiers were also measured and showed a capacitance of approximately 11 picofarads. Thus the total C_B is approximately 53 picofarads.

It should be noted that C_B forms a capacitance voltage divider with C_A which decreases the available signal voltage level to the input to the preamplifier. For this reason, every effort in design was made to minimize the value of C_B.

B. RADIOMETER ELECTRONICS

1. General Operation

The system block diagram is shown in Figure 1. This diagram illustrates the interrelationships between various portions of the radiometer electronics. The antenna assembly was discussed in section A.

The receiving system consists of a stepping superheterodyne receiver with a center frequency tunable from 50 kHz to 3.53 MHz in eight steps, a noise calibrator, an associated power supply, and an antenna.

Antenna signals are first amplified by a pair of low-noise broadband preamplifiers. The preamplifier inputs are filtered to prevent telemetry signals from entering the radiometer. The antenna and input circuits are untuned.

The preamplifier outputs, one of which is inverted, are summed in an RF summing amplifier. The summing amplifier contains a low pass filter to reject undesired frequencies above 3.53 MHz.

The output of the summing amplifier is mixed with a crystal-controlled, stepped-frequency local oscillator signal to achieve the tuning in eight steps across the frequency band with center frequencies from 50 kHz to 3.53 MHz. An analog voltage is generated in the oscillator circuitry to identify the operating center frequency. Frequency stepping is synchronized with the data system.

The IF amplifier is gain-controlled (AGC) with a response that is logarithmic and has a useful dynamic range of 55 db. The IF bandwidth of 10 kHz (6 db) is determined by a crystal filter in the output of the mixer stage.

Following the IF amplifier is an envelope detector, the output of which is filtered to obtain a post-detection time constant of 0.12 seconds.

A solid state noise calibrator is periodically switched to one of the preamplifier inputs with the antennas disconnected for calibration purposes. The input of the other preamplifier is terminated in a dummy antenna during the calibration period. Alternate preamplifiers are selected at each calibration cycle. The antenna relay and the calibration level-controlling relays are controlled by spacecraft timing signals. An analog voltage corresponding to the levels used for calibration is generated and fed to the spacecraft data system. Calibration occurs every 2.91 hours.

Figure 3 shows the voltages or signals required or expected at the radiometer's interfacing connectors.

The experiment blivet and covers are magnesium with selective gold plating to improve the electrical conductivity. The outside of the main experiment package is painted black with the exception of the base plate which is gold for good electrical and thermal conductivity. See Figures 4 and 5.

The mechanical layout of the main experiment package is shown in Figure 6. The outside dimensions of the package are 7.25" x 7.0" x 4.8". The package mounts on the spacecraft by four (4) 10-32 bolts.

The main experiment package dissipates approximately 2.0 watts over a baseplate area of 49.1 square inches. This gives a power density of approximately 0.04 watts per square inch. There are no local hot spots that are likely to cause difficulty.

The radiometer operates on a continuous duty cycle, being turned on and off only by ground commands. The average power consumption for the entire experiment (preamplifiers and main experiment package) is approximately 2.5 watts. A peak of approximately 5.0 watts is required during the calibration cycle (every 2.91 hours). The power profile for the experiment is illusrated in Figure 7.

2. Timing

The sequence of events in the radiometer is illustrated in Figure 8. Line A shows the C17 clock pulses furnished by the spacecraft, recurring at 0.64 second intervals. This is the repetition rate of the spacecraft data frame at the low bit rate and occurs 0.60 seconds before the data sampling time shown in line C. Each pulse causes the radiometer frequency to change as shown in line B. The eight frequency steps, F1 through F8, constitute a subcycle of approximately 5.12 seconds.

One data sample is taken during each frequency step at the low bit rate. At the high bit rate four (4) data samples are taken during the same period. Frequency Identification voltages replace the radiometer output voltages for the first sequence in each telemetry page (1/16 of the page).

The frequency stepping subcycle repeats continuously except in the event of a ground command to disable the automatic frequency stepping.

The calibration cycle consists of sixteen subcycles of eight frequency steps each as shown in line B' (same as line B except drawn to a smaller time scale). The noise calibrator level, as shown in line D', is held constant during the first subcycle. Thus all eight frequencies are calibrated at the same level. This is repeated for the next three subcycles at successively decreasing calibrator output levels. This calibration subcycle is repeated three additional times until each frequency has been calibrated four times at each calibration level. At the end of the 81.92 second calibration period, the calibrator is disconnected and the antennas are reconnected to the preamplifier inputs.

The calibration occurs only once every 2.91 hours. This is shown in line D". The antenna is connected to the radiometer for the remainder of the time (approximately 99.2% of the time). Action of the antenna relay is illustrated in line E".

3. Preamplifier

3.1 System Sensitivity

The system sensitivity of the radiometer was optimized for use with a 150 dipole* and a broadband untuned input circuit.[1,2,3,4,5]

The outline below summarizes the steps followed in the development of the system:

(a) Selection of a low noise transistor for the input stage. A 2N5397 was selected for this application.

(b) Selection of the best circuit configuration consistent with the lowest noise figure and other system requirements, mainly high input impedance. A common source configuration was chosen for the input stage.

(c) Determination of the four noise parameter F_o, R_n, G_o, and B_o,[6] and their variation with operating point.[7,8]

(d) Calculation of the $R_R T_R$ product with the specified values of C_A = 137.5 picofarads and C_B = 45 picofarads. The following equation was used:

$$R_R T_R = R_R T_o (F_o - 1) + \frac{R_R R_n T_o}{G_S} \left((G_s - G_o)^2 + (B_s + B_B - B_o)^2 \right)$$

---

* The dipole was originally designed to have a half-length of 150 feet but due to a failure in the deployment mechanism, the actual length is 80 feet. The effect of this reduced antenna length on the system operation is indicated on the applicable plots.

where:

R_R = Equivalent source resistance (antenna radiation resistance)

T_o = 290° K reference temperature

T_R = Effective receiver input noise temperature

G_s = Equivalent shunt conductance of the source

B_s = Equivalent shunt susceptance of the source

B_B = Shunt susceptance due to C_B

F_o, R_n, G_o, and B_o are the noise parameters of the system.

(e) Laboratory measurements were made on the final system using a broadband noise source and an equivalent dummy antenna. Data obtained was compared with the computed values of $R_R T_R$ and the correlation was very good.

(f) Using values of $R_R T_R$ found experimentally for C_A = 137.5 picofarads and C_B = 45 picofarads, the values of T_R for the eight operating frequencies were computed by dividing by the computed values of R_R found for the antenna using:

$$R_R = 80\,{}^2(h/\lambda)^2$$

where (h/λ) is the half-length of the dipole in wavelenths. This equation is accurate within a few percent for $(h/\lambda) < 0.1$ and is a reasonable appr oximation to the actual antenna radiation resistance.

(g) The tangential temperature T_T (minimum detectable signal), was then found from the equation:

$$T_T = \frac{5T_R}{\sqrt{B\tau}}$$

where:

B = Receiver bandwidth in Hertz (10^4 for this radiometer)

τ = Post-detection filter time constant in seconds (0.12 seconds)

The factor of 5 is an arbitrary factor arising from the ratio of frequency peak to rms values of the output, and is based on observational experience.

The system tangential temperature, T_T, is shown plotted for both an 80 foot and 150 foot dipole on an anticipated cosmic background brightness model in Figure 9. The data points are those observed in the UM/RAO 1962 and 1965 rocket experiments.[9,10]

Further increases in system sensitivity can be realized by appropriate averaging in the data reduction program, provided the phenomena being studied are either stationary or varying considerably slower than the data rate. If N independent samples are averaged, the sensitivity can be increased by a factor of $\sqrt{N}$.

3.2 Preamplifier Circuit

Figure 10 is a circuit diagram of one of the low noise RF preamplfiers. A four section resistor-distributed capacitance filter on the input of the preamplifier prevents signals picked up on the antennas from the spacecraft telemetry transmitters from entering the radiometer.

Q1 is an FET connected as a common source amplifier, yielding a good noise figure and reasonably high input impedance. Q2 and Q3 are bootstrap amplifiers to further increase the input impedance of the preamplifier. This high input impedance is a spacecraft requirement since there are four preamplifiers sharing the same antenna.

Q4 is a unity gain phase splitter, allowing C7 to be connected to either output depending on whether the preamplifier is to be connected as an inverting or non-inverting preamplifier.

Q5 through Q8 comprise a push-pull complementary amplifier having a very low output impedance. The low output impedance is necessary since the preamplifier must drive a rather long coaxial cable between the preamplifier and the main electronics package.

The preamplifier has its own voltage regulator to filter out any noise that may be picked up on the +18 volt buss between the main experiment package and the preamplifier. Monitor outputs on the preamplifier zener voltage, preamplifier temperature, and calibration relay are also included in the regulator portion of the preamplifier electronics.

4. RF Summing Amplifier

The RF summing amplifier is shown in Figure 11. The outputs of the two preamplifiers are summed at the base of Q102. Since one of the preamplifiers produces an inverted output, and a signal impinging on the dipole antenna pair from distant sources will produce voltages in the two antennas which are out of phase with one another, the two signals will be additive in the summing amplifier. For signals generated locally, however, (spacecraft interference) the voltages on the antennas will be in phase and will therefore cancel in the summing amplifier.

A Chebyshev low-pass filter is incorporated between the first and second stage of the amplifier. This filter has an in-band ripple of 0.1 db., is 3 db down at 4.1 MHz, and 75 db down at 10.7 MHz. This filter serves three purposes:

(a) Rejection of spurious responses, notably at the IF and image frequencies.

(b) Rejection of the self-noise produced at spurious frequencies, thus improving the overall noise figure of the system.

(c) Suppression of radiation at the local oscillator frequencies (10.75 to 14.23 MHz) from the receiving antennas.

The filter is followed by Q103 which is an emitter follower with a low output impedance suitable for driving the mixer stage. Both stages are biased for low DC drift and degenerated for stabilized gain.

The voltage gain of the amplifier from the base of Q102 to the output of Q103 is approximately 14 db. However, an attenuation of approximately 21 db is provided in the summing network preceding Q102, giving a net gain of -7 db. The purpose for this is two-fold:

(a) This experiment was originally designed for the OGO-V spacecraft which had a much shorter antenna and therefore some means of reducing the overall system gain was found necessary. The input to the summing amplifier seemed the most logical place to put the attenuation since this would also attenuate any interference generated between the preamplifiers and the main electronics package inside the spacecraft.

(b) The use of attenuation in the summing network prevents signals being fed from the output of one preamplifier back to the output of the other preamplifier.

An additional resistor was included in the attenuator circuit, shunted by a cuttable jumper. This resistor was included so that if the IMP spacecraft proved to have a higher than anticipated RFI level, the overall system sensitivity could be reduced an additional 15 db. Happily, this did not prove to be the case and the jumpers were flown intact.

The series output inductor is an additional RFI filter and was added as a result of RFI tests conducted on the OGO-V radiometer. This inductor markedly reduces the susceptibility of the radiometer to both conducted and radiated interference outside the frequencies of interest.

5. Mixer and Crystal Filter

The mixer, crystal filter, and drivers are shown in Figure 12.

The mixer is a balanced diode type which feeds directly into a driver stage. The collector load of the driver stage is a crystal filter having a center frequency of 10.7 MHz. The driver stage and the stage following the crystal filter provide termination for the filter so that maximum flatness is achieved in the passband.

The crystal filter is the element which determines the IF bandwidth. The specifications for the filter are as follows:

Center Frequency	10.7000 ± 0.005 MHz
Bandwidth	10.0 ± 0.05 kHz (6 db) 24.0 ± 1.5 kHz (60 db)
Passband Ripple	1.0 db Maximum
Insertion Loss	2.0 db Maximum
Spurious Response Rejection	80 db Minimum

(From 1.0 MHz to the lower 80 db point, and from the upper 80 db point to 40 MHz)

The crystal filter stage has an emitter follower output, providing a low output impedance for driving the IF amplifier. This eliminates the problem of driving the variable input impedance of the IF amplifier, reduces pickup in the IF amplifier input cable, and simplifies adjustment of the matching termination for the crystal filter.

6. Logic

6.1 General Operation

The basic logic used to generate the timing sequence is shown in Figures 13 and 14. A timing signal from the spacecraft (see Section 2) enters the Pulse Drive Redundancy (PDR) circuit every 0.64 seconds in normal operation. A pulse suitable for driving the oscillator switching flip-flops is produced at the output of the PDR at this same rate. At the same time, a second pulse checking network is pulsed every 5.12 seconds (C21). This pulse is used to reset the oscillator switching logic when the experiment is first turned on.

The oscillator switching flip-flop chain has a scale of 2^3 (= 8) and applies DC power to the local oscillators in the proper sequence through suitable gates and drivers. The flip-flops are AC coupled and were designed to have good temperature stability and noise immunity.

On occasion it may be desired to operate the radiometer at a fixed frequency for an extended period of time. For this reason an automatic stepping disable relay was incorporated into the system. This single frequency step circuitry is illustrated in Figure 14.

The stepping disable relay is a latching type which requires only a 30 millisecond pulse to change state. A ground command (63T) energizes Relay RY601 (Figure 13) which disables the normal frequency stepping and allows the appropriate frequency of operation to be selected. The calibration sequence is not affected by this mode of operation but only the selected frequency will be calibrated.

The desired frequency of operation may now be selected through the use of a second ground command (62T) which provides a pulse input to the oscillator switching logic, bypassing the PDR circuitry. A single pulse is produced each time the ground command is sent so that individual frequencies are easily selected. Q609 was incorporated in the circuit because the logic flip-flops were originally designed for a negative going pulse of approximately 18 volts magnitude. The IMP spacecraft produces positive going pulses of approximately 7.5 volts magnitude. Q609 is used as an inverter to produce the proper polarity and magnitude pulse for for the logic upon issuance of the single step ground command.

A third ground command (60T) returns the input of the oscillator switching logic to the output of the PDR circuit when it is desired to return to the normal frequency stepping mode of operation. This ground command latches RY601 in the normal position and it will remain in this position until another disabling command is sent.

6.2 Pulse Drive Redundancy (PDR) Circuit

The Pulse Drive Redundancy (PDR) circuit is shown in Figure 13. Its purpose is to maintain sequential operation of the radiometer in the event the spacecraft timing pulse falls below specifications, becomes intermittent, or fails completely. The characteristics of the timing pulse were discussed in Section 2 and will not be repeated here.

The first stage of the PDR circuit is an emitter follower which isolates the Schmitt Trigger (Q402 and Q403) from the spacecraft timing signal. This is necessary in order to keep the input impedance high independent of the state of the Schmitt Trigger.

The Schmitt Trigger produces an output pulse whenever the pulse level from the emitter follower exceeds a predetermined level. This output feeds both a free-running multivibrator (Q404 and Q405) and one input of a two input OR gate (D401 and D402).

The free-running multivibrator is synchronized with the Schmitt Trigger output pulse in such a way that its output pulse is in phase with the Schmitt Trigger pulse. This multivibrator output pulse forms the other input to the two input OR gate and is fed to the oscillator switching logic timing chain.

The PDR circuit will produce pulses at the free-running multivibrator rate in the event of failure of the spacecraft timing signal. This rate was set at approximately 1.26 seconds per pulse. This rate, which is approximately half the normal timing rate, was chosen so that at least half the data samples taken would be useful for data reduction. What this means is that at least half the data samples would have been taken at a sufficient number of radiometer time constants after frequency switching to be useful.

Note that thermistor R414 (figure 13) has been jumpered. This was done to change the PDR rate from its rate as designed for the OGO spacecraft to the rate required for the IMP spacecraft. It was found to be simpler to jumper this thermistor than to remove it.

6.3 Oscillator Switching Synchronizing Circuit

The Oscillator Switching Synchronizing circuit, shown in Figure 13, consists of transistors Q453 - Q455 and a distribution matrix consisting of resistors R463 - R468 and diodes D453 - D455. Q453 - Q455 comprise an emitter follower and Schmitt Trigger stage identical with the one used in the PDR circuit. Each time a C21 spacecraft timing signal arrives, a pulse is generated by the Schmitt Trigger and fed to the distribution matrix. Note that the C21 input pulse is disabled at the same time that frequency stepping is disabled (Figure 13) for the fixed frequency operation. If this were not done the oscillators would be reset to the first frequency (50 kHz) every 5.12 seconds even though the single frequency mode had been commanded.

The outputs from diodes D453 - D455 are fed to the oscillator switching logic flip-flops shown in Figure 15. The signals are fed to the reset input on each of the three flip-flops, placing them in the reset state if they are not already in that state. This pulse is coincident with the 0.64 seconds per pulse C17 timing signal and occurs once every eight C17 pulses. Thus, once the synchronizing signal initially resets all the flip-flops, the next occurrence of the pulse will find the flip-flops in the reset state and no response to the pulse will occur.

6.4 Oscillator Switching Logic

The logic which determines which of the eight oscillators is operating at any given time is illustrated in Figure 15. The logic consists of a three-stage counter, a diode matrix, and eight power switches controlled such that only one oscillator is powered at a time.

6.5 Calibration Control

The Calibration Control circuitry is shown in Figures 13, 14, and 16. These correspond to the schematics for boards 4, 6 and 7 in the Main Electronics Package.

In Figure 14, emitter follower Q610 serves to isolate the spacecraft calibration signal (Cal) from the several circuits which are controlled by this signal. Q610, in combination with D615 and D616, provides one input to two two-input AND gates which combine the Cal signal with the spacecraft C21 and C22 timing signals. The outputs from these AND gates are true <u>only</u> if Cal <u>and</u> C21 are both true or Cal <u>and</u> C22 are both true. The use of these signals will be discussed later.

The Cal signal buffer also drives two additional circuits. The first of these is a latching relay circuit (RY602). The function of this relay is to direct the output from the noise calibrator to the input of one of the two preamplifiers. Each time the radiometer is calibrated this relay changes states, thereby calibrating a different preamplifier. Thus, it takes two calibration periods to calibrate both preamplifiers. A signal is also taken from one of the contacts on the calibration relay and fed to the Aliveness/Cal telemetry word (APP-11). This voltage level uniquely identifies which of the two preamplifiers is being calibrated during a particular calibration period. This relay circuit is shown in Figure 14.

The other circuit fed by the Cal signal buffer is the relay driver circuit for RY451 (Figure 13). This relay serves two functions: it supplies +28 volt power to the relays in the preamplifier modules which switch the preamplifier inputs from the antennas to the noise calibrator circuitry; and it changes the voltage level on the FID/CAL telemetry word to identify the calibration period.

The purpose of the Cal, C21, and C22 signal voltages previously described is to drive the calibration control relays. These relays, along with their associated drivers, are shown in Figure 16.

In the discussion to follow it should be realized that the Cal signal is true for the entire calibration period so the outputs of the AND gates previously described are controlled entirely by the levels of the C21 and C22 signals. With this understood, the operation of the calibration relays is as follows:

(a) When C21 and C22 are both true, which occurs at the beginning of each calibration cycle, both relay RY751 and RY752 are energized. This causes the maximum noise output from the calibrator to be applied to the selected preamplifier. At the same time, the second set of relay contacts feeds a DC voltage to the telemetry system which indicates the calibrator noise level.

(b) When C21 goes false and C22 remains true, the next lowest calibration signal level is selected. Another DC voltage is fed to the telemetry, indicating the new calibration level.

(c) When C21 becomes true again and C22 goes false, the second lowest calibration level is selected and an appropriate DC voltage is fed to the telemetry system.

(d) When both C21 and C22 are false but the Cal signal remains true, a "no noise" condition is selected. During this period no calibrator noise is being fed to the preamplifiers but they are both still connected to dummy antennas. Therefore, the output of the radiometer is a measure of the internal noise of the system. The DC voltage fed to the telemetry system is the same as the indication for the third level. This is due to a limitation on the relay contacts.

NOTE: Although DC voltages are generated which identify the different levels of calibration signal level, only the indication for the highest level appears in the telemetry data. This is due to a restriction on the multiplexing of this information with the radiometer output data.

A calibration cycle (four levels) requires 20.48 seconds and is repeated four times during each calibration period for a total of 81.92 seconds. A calibration period will occur every 2.91 hours during normal spacecraft operation.

7. Local Oscillators

Eight crystal-controlled oscillators are used in the radiometer with frequencies ranging from 10.75 to 14.23 MHz. The circuits for four of the eight oscillators are illustrated in Figure 17. The other four circuits are identical with the exceptions noted on the drawing. This circuit was developed to require neither inductive elements nor critical adjustments. This allows a single circuit to be used for all eight crystals with little or no individual adjustment. This also allows the operating frequencies of the radiometer to be changed at any time, within the 50 kHz to 3.53 MHz spectrum, by simply changing a crystal.

The circuit, which was designed for high stability of both the output frequency and amplitude, consists of a slightly degenerated common emitter feedback amplifier with the crystal element in the feedback path. This circuit provides both low drive voltage to the crystal and a low output impedance with a good waveform at the emitter. This point is coupled through a switching diode to a common output buss.

The oscillator which is selected by the logic has +11.2 volts applied to its input while all the other oscillators' power inputs are grounded. This causes the selected oscillator to operate while the others are de-energized.

Diode switching is used between the oscillator circuits and the common output buss so that the inactive oscillator circuits will not load the active oscillator output. Current through the selected diode reduces its dynamic impedance to a low value (nominally 25 to 30 ohms) and raises the DC level on the common output buss to a values of from approximately 1.5 to 4.0 volts depending on the circuit selected. This will be discussed later under frequency identification. Since all the power inputs to the unselected oscillator circuits are grounded, the diodes in these circuits are back-biased by the DC level of the output buss. In this condition the capacity of each diode is approximately 1.5 pf., giving a total capacitive loading of approximately 10.5 pf. on the common output buss. This impedance does not represent an appreciable loading of the buss even at the highest oscillator frequency (14.23 MHz).

The power is switched from the previous selected circuit to the new circut when a new frequency is selected by the logic. The RF buildup time to produce a fully stable output is 3 to 8 milliseconds after power is applied to an oscillator circuit. The oscillator output decays to zero in less than 1 millisecond when power is removed from a circuit.

An analog voltage is generated and fed to the telemetry system so that the frequency of operation of the radiometer is identified. The means of generating this voltage is a resistor in the oscillator circuit which is in series with the output switching diode. The value of the resistor determines the current through the diode and thus the DC voltage level on the common output buss (see above). This DC level is fed to the telemetry system and uniquely determines the frequency of operation.

8. IF Amplifier and Detector

The specifications for the IMP-I IF amplifier were defined as follows:

(a) The amplifier should be gain-controlled (AGC) with a logarithmic response $\pm$ 1 db over a 40 db range of input signal and should have a 55 db useful range.

(b) Maximum small signal voltage gain from amplifier input to envelope detector input of 70 db (approximately).

(c) DC output range of from 0.05 volts (no signal) to +4.9 volts (maximum signal).

(d) DC output impedance < 1000 ohms.

(e) Center frequency - 10.70 MHz.

(f) Bandwidth - 400 to 600 kHz between 3 db points.

(g) No-signal output variation < 0.06 volts for a temperature range of -10°C to +50°C.

(h) Dynamic temperature stability of < 3 db variation in input signal for the same output signal over a range of -10°C to +50°C.

(i) Center frequency shift with both temperature and signal level should be small enough so that the gain at 10.70 MHz is no less than 0.95 maximum gain.

Extensive research was conducted to design an amplifier which met all of these requirements. The result is illustrated in Figure 18.

Of all the AGC principles investigated, the most successful was the use of a variable impedance element in the emitter circuit of a common emitter amplifier. This allows the gain variation of the stage to be controlled by the emitter current.

Certain types of germanium diodes show a wide variation in forward resistance with diode current while displaying a very low temperature coefficient of resistance with varying current. Typical values of forward resistance for the 1N498 diode are as follows:

DIODE CURRENT Microamperes	FORWARD RESISTANCE Ohms
50	805
100	450
250	198
500	108
1000	59

As the AGC voltage is varied, a varying emitter current will flow through the diode, modulating its resistance according to the table above. Gain variations of over 30 db per stage can be obtained using this method with well controlled logarithmic response of over 20 db per stage.

A four stage, AGC amplifier having two variable gain stages, one of which is a cascode stage, was designed and built for the IMP-I (OGO-V) radiometer. In addition to being gain-controlled it is temperature compensated at a critical point with a sensistor. This amplifier fulfills all the requirements set forth above as being necessary for proper overall system operation.

Following the IF amplifier is an envelope detector, the DC bias of which is stabilized by a sensistor. The output of the detector is fed to an emitter follower amplifier. The AGC voltage for the IF amplifier is developed in the emitter circuit of this amplifier and is fed back to the first two stages of the amplifier for gain control.

The drive for the final output driver stage is developed in the same emitter circuit. The elements which determine the post-detection time constant (τ) of 0.12 seconds are located between this emitter follower and the final driver stage.

The radiometer output voltage which is fed to the spacecraft telemetry system is developed in the emitter circuit of the final driver stage. The output voltage is constrained to be between 0.0 and +5.1 volts by the combination of D207 and D208 which determine the emitter bias and collector voltage respectively. This constraint satisfies the requirements of the telemetry system on the IMP-I spacecraft.

9. Inflight Calibrator

A solid-state noise generator is used so that the radiometer can be calibrated in flight during the previously discussed calibration period. This noise calibrator circuitry is illusrated in Figure 16.

Solid-state noise diodes with well known noise properties were investigated for use and life test data was collected on ten units for more than two years. In all cases it was found that the noise properties of these diodes (noise spectrum, absolute output level, and temperature coefficient of noise output) remained constant provided they were supplied from a constant current source. In only one case did the noise properties of a diode change during the life test, and this was accompanied by a current change very early in the life test.

The circuit incorporating the noise diode and the associated video amplifier was designed to produce a maximum RT product of approximately 7.55×10^{10} Ω°K. The response of the video amplifier is flat (± 0.1 db) from 20 KHz to 1.2 MHz and is 3 db down at approximately 4.0 MHz. The overall gain of the amplifier is approximately 12 db. The amplifier is temperature compensated at critical points and uses degenerative feedback to achieve a high degree of gain stability.

The noise spectrum of the diode is essentially "white" to well beyond the cutoff frequency of the video amplifier and thus does not influence the overall noise spectrum presented to the radiometer input during calibration.

To monitor the current through the noise diode during flight, since this is the critical parameter in determining the noise output of the diode, a series resistor provides a voltage drop which is fed to the telemetry system. This voltage is one of the experiment's Performance Parameters (APP-16) and provides continuing information on the diode current during flight.

A temperature-sensitive network consisting of a thermistor-resistor combination is incorporated into the noise amplifier circuitry to provide inflight information about the noise diode temperature. The output of the thermistor bridge is fed to the telemetry system (PP-5). The calibration for this bridge is shown in Figure 20.

It should be noted that the solid state noise diode was not the primary standard for calibration of the radiometer. The primary standard is a thermionic diode noise source which was used during the laboratory calibration of the radiometer. This will be covered under the section on preflight calibration. The only purpose of the inflight calibrator is to determine the magnitude of any gain changes that may occur in the radiometer during flight.

A four-level calibration is used to achieve adequate calibration of the radiometer at all frequencies. The calibration cycle consists of four (4) frequency subcycles (see Sections 2. and 6.5), each having a 5.12 second duration. During the first subcycle the noise calibration signal is maximum and the preamplifier inputs are switched from the antennas to internal dummy antennas. The noise signal is injected into one of the preamplifiers while the other is terminated in the dummy antenna. During the second subcycle, a lower calibration signal level is injected. During the third subcycle, a still lower signal level is injected. During the fourth subcycle, no noise is injected but the preamplifiers remain connected to the dummy antennas. This is a measure of the internal noise of the system. This calibration cycle is repeated four times during each calibration period for a total of 81.92 seconds every 2.91 hours. At the end of the four calibration cycles, the antenna relays restore the antennas to the preamplifier inputs and the calibration control relays are restored to their original states. The only relay which remains in the same state until the next calibration period is the relay that determines which of the preamplifiers will be calibrated during the next calibration period.

10. Voltage Regulator

One of the most important considerations in the design of a highly sensitive radio frequency radiometer is the minimizing of radio frequency interference (RFI) generating circuitry. While filtering can be used to adequately reduce external RFI, internally-generated RFI is much more difficult to eliminate. For this reason the choice of design for the radiometer power supply becomes extremely important. The basic choice is between a converter-type power supply and a series regulator.

A converter power supply has three main advantages:

(a) It provides good input/output isolation.

(b) It is efficient.

(c) It can provide a dual polarity voltage higher than the input voltage.

On the other hand, a converter has two major disadvantages for use with a satellite-borne radio astronomy receiver:

(a) The circuit is more complex, calling for more components, reducing the overall reliability figure.

(b) The circuit lends itself to generation of a large amount of RFI.

Since the IMP radiometer uses single polarity low voltage circuits exclusively, a careful design can provide adequate input/output isolation from a series regulator, as well as approximately the same efficiency as a converter, we chose the series regulator circuit, primarily for RFI reduction.

The specifications for the series regulator are as follows:

Input Voltage Range

Continuously	+23.5 to +33.5 volts DC
Intermittently (Up to 10 minutes)	0 to +42.0 volts
Transient Tolerance (10 milliseconds maximum)	+50.0 volts

Line Regulation (23.5 to 33.5 volts)	$< 0.1\%$
Load Regulation (0 to 124 ma)	$< 0.1\%$
Temperature Coefficient (-20°C to +60°C)	$< 0.01\%/°C$

NOTE: The specification for the continuously applied input voltage range was dictated by the OGO-V spacecraft requirements for which this instrument was originally designed. This is a much more stringent specification than that specified for the IMP-I spacecraft.

It should be pointed out that these regulation figures are not the actual figures for voltage regulation at the individual circuits since all the critical circuits have temperature-compensated zener diodes on the circuit boards to provide additional requlation. Thus a realistic figure for the regulation at the critical circuits is 0.01% for all line and load conditions over a temperature range of -10°C to +30°C.

The regulator circuit is shown in Figure 19. C323 forms a low impedance path for noise on the spacecraft supply and prevents it from entering the regulator circuit. It also filters out noise generated in the regulator and keeps it from being reflected onto the spacecraft power buss.

Q301 and Q302 form a Darlington pair amplifier with Q301 being the series control element in the regulator circuit. The control voltage to the base of Q302 comes from the output of the sense amplifier, Q304 and Q305. The input to this sense amplifier is the output voltage-sensing network consisting of R309, R310, R311 and R313. R309 is a sensistor which improves the temperature coefficient of the regulator. There is also a sensistor in the emitter circuit of Q305 which, in combination with D302, sets the operating point for the first stage of the sense amplifier. Again, this sensistor at the critical first stage increases the temperature stability of the regulator circuit. D303, in the emitter circuit of Q304, sets the operating point for the second stage of the sense amplifier.

R312 and R314 form a voltage divider which senses the output voltage and feeds this level to the telemetry system for monitoring purposes during flight (APP-11).

Current limiting circuitry was incorporated to protect the series pass transistor from transient or accidental shorts. The circuit consists of R304, D301, and Q303. When the voltage drop across R304 exceeds the threshold voltage of D301 in series with the base-emitter junction of Q303, Q303 conducts, lowering the base drive to Q302. This increases the collector-emitter drop across Q301 and rapidly drives the regulator output voltage to zero.

Special precautions were taken to reduce the conduction of RF noise from the regulator to the RF circuits and also between RF circuits. D302 was bypassed so that any noise generated in this zener would not be introduced onto the buss voltage. A high degree of decoupling between critical boards was accomplished by using LC filter networks in addition to the low AC impedance presented by the zeners. This effectively isolates the circuits from each other and reduces the interchange of RFI.

Also illustrated in Figure 19 are the LC line filters. These serve the dual purpose of reducing external RFI conducted into the experiment and reducing the level of internally-generated RFI conducted out of the experiment into the spacecraft wiring.

A temperature sensing network consisting of R302, R303 and R305 was incorporated so that the temperature of the series pass transistor could monitored. This monitor would give an indication of abnormal power dissipation in the series transistor and allow shutting off the radiometer before serious damage was done to the regulator. The calibration of this network is shown in Figure 20. The output of the network is fed to the Test Interface Connector (J102) for preflight monitoring. There is no provision for inflight monitoring of this temperature.

C. GROUND SUPPORT EQUIPMENT

1. General Operation

The Ground Support Equipment (GSE) was designed to operate and checkout the UM/RAO radiometer experiment for the IMP-I spacecraft before, during, and after various qualification tests. The GSE consists of three (3) suitcase-mounted modules.[11] These modules are designed as follows:

(1) Test Monitoring Module (Suitcase "A").

(2) Spacecraft Simulator Module (Suitcase "B").

(3) Stimulus Module (Suitcase "C").

Four test modes are possible with the GSE. The principal test mode consists of controlling, dynamically stimulating, and monitoring the experiment. This mode requires the use of Suitcase "A", Suitcase "B", and Suitcase "C".

The second test mode consists of powering and monitoring the experiment while the package is separated from the spacecraft and no connection is made to the Spacecraft Interface Connector. In this mode the radiometer changes frequency at its internal free-run repetition rate (1 step/1.2 seconds). This mode requires only Suitcase "A".

The third test mode controls the experiment's internal calibration cycle while the package is on the spacecraft. This test mode allows internal calibration of the experiment to take place as often as desired, rather than at the spacecraft rate of once every 2.91 hours. An adjunct to Suitcase "A", the Calibration Control and Auxiliary Voltage Monitor Box, is required for this test mode.

The fourth test mode consists of dynamically stimulating the experiment while it is integrated into the spacecraft. This mode requires the use of only Suitcase "C".

2. Test Monitoring Module (Suitcase "A")

Suitcase "A" provides a means for monitoring the voltages that are normally fed to the spacecraft telemetry system. This monitoring is accomplished via a cable connecting the suitcase to the package at the Spacecraft Interface Connector. In addition, the suitcase can monitor the experiment supply voltage, the +18 V internal regulator voltage, and, through the Test Interface Connector, four voltages associated with the EFM preamplifiers.

Suitcase "A" contains an auxiliary experiment power supply, a digital voltmeter (DVM), and the necessary switching to select and display any one of the test signals from the radiometer. The +28 V power supply in Suitcase "A" is not used if the suitcase is used in conjunction with Suitcase "B".

An adjunct to Suitcase "A", the Calibration Control and Auxiliary Voltage Monitor Box, provides a means for controlling the internal calibration of the radiometer.

Figure 21 is a block diagram of the Test Monitoring Module. The test point selector switches the test point voltage to be applied to the DVM input. Any one of the twelve (12) test points may be selected by the main switch and four (4) test points may be selected by the auxiliary switch.

The DVM switch selects the input to the DVM. In either Test Point position it is connected to one of the test point selector switches. In the External position it is connected to the binding posts on the front panel. In the S/C Voltage position it is connected to the +28 V supply buss and reads the voltage applied to the experiment from either Suitcase "A" or Suitcase "B".

A key-lock switch activiates the auxiliary +28V power supply to power the experiment package when Suitcase "B" is not connected to the package.

The circuit diagram for Suitcase "A" is shown in Figure 22.

3. Spacecraft Simulator Module (Suitcase "B")

The Spacecraft Simulator Module supplies all the signals and power normally supplied to the radiometer by the spacecraft. The module is connected to the radiometer by a cable which mates with the Spacecraft Interface Connector J101.

Figure 23 is a block diagram of the Spacecraft Simulator Module.

Operating the AC key-lock switch applies power to the adjustable power supply and to the power supplies (+6 V, -6 V, +18 V, and +28 V) which are required for the suitcase electronics. The Electronics On switch simulates the radiometer electronics On/Off command.

The 30 milliseconds commands are sent by energizing the command line selected by the Impulse Command Select switch for 30 milliseconds. The operation is accomplished by the Impulse Command circuitry in the following manner: The Reset pushbutton resets two flip-flops, arming the Command pushbutton. Two lamp drivers are driven by the flip-flops and indicate the armed condition by turning the Reset light on and the Command light off. Pressing the Command pushbutton causes Flip-Flop 2 to go to the set condition which starts the 30 millisecond One-Shot and turns the Reset Light off. The One-Shot pulse output causes the Relay Driver to energize the Impulse Command relay for 30 milliseconds. The voltage across the relay coil is fed to the Command Signal Buffer and from there through the selected command line.

The Impulse Command relay, in returning to the de-energized state, sets Flip-Flop 1 which in turn causes the Command light to come on. When this light comes on, the operator is assured that the Impulse Command relay has operated properly. Flip-Flop 2 operates as a lock-out and assures the operator that only one command will be sent each time he completes the Reset-Command sequence.

The clock signals are generated by a master clock operating at a basic rate of one (1) pulse/0.64 seconds, followed by nine binary dividers to provide pulses corresponding to the C_{17}, C_{21}, C_{22} timing signals from the spacecraft as well as a calibration clock signal. The calibration cycle provided by this system is 40.96 seconds long instead of the 81.92 second cycle provided on the spacecraft, and it occurs every 5.46 minutes instead of 2.91 hours. Since spacecraft specifications call for relatively long propagation delays between clock pulses, Schmitt Trigger delays were introduced between each timing signal to simulate the delay time. Clock pulse height is adjustable from 0 to +9.5 volts by varying R55 and is normally set at 7.5 volts as indicated on the front panel meter. Clock outputs are buffered to make them appear to the experiment to have the same impedance as the spacecraft clock lines.

Circuit diagrams for Suitcase "B" are shown in Figures 24 and 25.

4. Stimulus Module (Suitcase "C")

Suitcase "C" contains a temperature-limited diode, a video amplifier, and associated power supplies which comprise a noise source for simulating the cosmic noise input to the radiometer. The suitcase also contains a H-P 651A Test Oscillator for measuring the gain of the video amplifier.

Figure 26 is a block diagram of the Stimulus Module. The noise source consists of a temperature-limited diode followed by a four stage video amplifier. The value of diode current is set by adjusting the diode filament voltage furnished by the regulated filament supply.

The noise diode B+ supply furnishes power to the diode plate circuit and to the operational amplifier in the filament voltage regualtor.

The video amplifier power supply furnishes +18 volts for operation of the video amplifier.

The isolation transformer and filters provide 115 VAC, 0.2A for external use while "C" is operating, 1.04A when "C" is off.

The H-P 651A Test Oscillator is externally connected for calibration purposes.

The circuit diagram for Suitcase "C" is shown in Figure 27. The circuit diagram for the noise amplifier in the noise calibration source is shown in Figure 28.

III. PREFLIGHT CALIBRATION

A. GENERAL

The preflight calibration of the IMP-I radiometer can be divided into three categories:

(a) Determination of the input impedance of the radiometer at the eight operating frequencies.

(b) Determination of the parameters which define the noise figure of the radiometer at the eight operating frequencies.

(c) Measurement of the overall system response over the anticipated temperature and input signal operating ranges.

The first two sets of measurements were conducted at room temperature with the data recorded by hand. The last set of measurements was made using the UM/RAO Data Logger facility. This facility not only allowed automatic control of the radiometer but also produced a computer-compatible digital magnetic tape.

The tape was processed on the UM/RAO Scientific Data Systems (SDS) 930 Computer and produced both digital printout and Calcomp plots of the system response curve.

B. INPUT IMPEDANCE MEASUREMENT

The equipment setup for the determination of the radiometer's input impedance is shown in Figure 29. The generator was adjusted for an input signal of approximately 10 millivolts rms at the radiometer. The bridge was then adjusted for a null as indicated on the Collins receiver RF meter and the impedance indicated on the bridge noted. This measurement was repeated for each of the eight operating frequencies of the radiometer.

The components of the input impedance of the radiometer at the eight frequencies are shown in Table 1.

C. DETERMINATION OF NOISE PARAMETERS

The four noise parameters, F_o, R_N, B_o, G_o, were determined at each of the eight operating frequencies of the radiometer.[6,7]

D. OVERALL SYSTEM RESPONSE CALIBRATION

1. General

It was known from our experience with earlier radiometers that a large effort was involved in obtaining adequate preflight calibration. Therefore, we approached the calibration program through a study to determine the feasibility of using the UM/RAO Data Logger facility for the system response calibration. We used the prototype radiometer to resolve the interfacing problems and to prove the feasibility and desirability of using the facility for this program.

It became immediately evident from the preliminary tests that the man-hours of effort required for the calibration program would be drastically reduced. In addition, three major advantages are offered using the Data Logger over recording the data by hand:

(a) A large amount of human error is removed. This is because human operators are not required to make any tedious measurements and record large volumes of data.

(b) A much larger volume of data can be taken, allowing averaging of the samples. This allows more accuracy in the data recorded in a noisy environment.

(c) The fact that the output of the facility is a digital tape allows the data to be processed immediately using a computer program to produce plots of the system response. This type of presentation allows rapid evaluation of the adequacy of the calibration procedure.

The total time required to record eleven parameters, at 174 different noise and preamplifier configuration conditions for each of ten temperatures was approximately 25 hours. This did not include the time for the temperature chamber to stabilize. The stabilization time was approximately one hour for each temperature. The calibration program was completed in 40 man-hours. This is less than 25% of the normal time required to do a similar task by hand, based on our experience with earlier radiometers. This, in addition to the other advantages listed above, represented a significant improvement over similar programs on other radiometers.

2. Test Setup

The Data Logger facility consists of a SDS Model MU31-1 Multiplexer, a SDS Model AD20-14 Analog-to-Digital Converter, an Ampex Model TM4113-D Digital Tape Handling System and special sequence and control circuitry constructed in the UM/RAO Laboratory from Computer Control Company 1 MHz logic modules.

The multiplexer has 16 input channels with an input impedance of approximately 100 kΩ. The maximum switching rate for this model is 15 kHz. The acceptable input voltage range is between ± 10 volts.

The A-D converter converts each sample to a thirteen bit plus sign bit ditigal representation. Thirteen bits provide a resolution of better than one part in eight thousand. The conversion rate for this model is 13,300 samples per second. The Converter also includes sample-and-hold circuitry which provides a sample aperature of less than 1 microsecond.

The TM4113-D Tape Handling System is designed to read and write tapes that are compatible with the UM/RAO SDS 930 Computer. It can be operated at tape densities of either 200 or 556 characters per inch and tape speeds of either 30 or 60 inches per second. It uses 2400 foot reels of 1/2 inch magnetic tape.

In addition to the sequencing and control circuitry provided to control the Data Logger facility, control circuitry was built to automatically sequence the radiometer through its eight frequency steps. This circuitry stepped the radiometer and then provided a delay of approximately one second before the radiometer data was recorded. This delay allowed the radiometer output to fully stabilize before it was sampled.

The Data Logger facility is shown in Figure 20.

A block diagram of the calibration setup is shown in Figure 31.

The temperature chamber used for the calibration was an Associated Testing Laboratories Model SLHU-1-LC-1. This chamber is capable of providing any temperature between -75 and +220°C with a temperature control of ± 1.1°C after stabilization.

The external noise source used for the calibration was a broadband noise source designed and constructed at the UM/RAO Laboratory.[12] This generator is similar in design to the Suitcase C Unit.

The output of the noise generator was fed through a Weinschel Model 64A precision attenuator which allowed the attenuation of the noise signal to be set to 1 db with a precision of ± .03 db.

The ground support equipment (GSE) used was a Suitcase B Unit which provided power and the necessary impulse commands to exercise the radiometer. A complete description of this unit and its operation can be found in reference 11.

The junction box was built to provide an interface between the cable to the Spacecraft Interface Connector on the radiometer and the input cables to the Data Logger Facility. This box contains scaling resistor strings and the necessary interfacing connectors. The junction box also contained a means of defeating the normal calibration sequence in the radiometer so that the radiometer did not go into the calibration cycle during the test. This allowed the calibration as well as the frequency stepping to be controlled externally.

3. Radiometer Configuration

For all of the calibration runs, the radiometer was kept in the manual frequency stepping mode with the internal calibration sequencing disabled. The stepping of the radiometer circuitry was controlled by a switch closure whose timing was determined in the control logic circuitry of the Data Logger. This circuitry changed the radiometer frequency, provided a delay of approximately one second and then initiated the sequence to write the data samples on the magnetic tape.

The control of the radiometer's internal calibration cycle was accomplished through the use of the Calibration Control Box which operates in conjunction with Suitcase "A" and is connected to the Test Interface Connector on the Main Electronics Package. Through the use of this box, any of the internal calibration levels may be selected for an extended period of time. It is also possible to keep the radiometer from going through its internal calibration cycle through the use of this box. This allowed the use of an external calibration source for noise injection.

4. Calibration Results

As mentioned earlier, the output of the Data Logger facility is a digital tape. This tape was processed after each temperature run as a check on the calibration procedure. The average time from the end of the temperature run to digital printout for the complete run was approximately 30 minutes. An example of the digital printout is shown in Figure 32.

The plotting of the data was normally not done until a sufficient number of temperatures had been run to show temperature variations in the system response. If it were desired to plot the data immediately, a turn-around time comparable with the time for digital printout was possible.

The data plotting was done on a California Computer Products (Calcomp) plotter. This device was driven by a controller designed and constructed at the UM/RAO which interfaced with the SDS 930 computer.

An example of a Calcomp plot of the radiometer calibration data is shown in Figure 33.

REFERENCES

1. UM/RAO Technical Report 68-10, Instrumentation for Radio Astronomy Measurements Aboard the OGO-V Spacecraft, B.D. MacRae, 20 September 1968.

2. UM/RAO OGO-E Memo No. 105, "Influence of Antenna Length on the OGO-E System Sensitivity", R.G. Peltzer, 20 September 1967.

3. UM/RAO IMP-I Memo No. 34, "Frequency Assignment and Gain Reduction", R.G. Peltzer, 22 September 1969.

4. UM/RAO IMP-I Memo No. 39, "Dipole Antenna Impedance for H = 150 Feet and H = 200 Feet", R.G. Peltzer, 25 October 1970.

5. UM/RAO IMP-I Memo No. 40, "System Gain Considerations", R.G. Peltzer, 27 October 1970.

6. "IRE Standards on Method of Measuring Noise in Linear Twoports, 1959" and "Representation of Noise in Twoports", Proceedings of the IRE, Vol. 48, No. 1, 1960.

7. UM/RAO Technical Report No. 64-9, A Simplified Representation of the Noise Factor of Junction Transistors, B.G. Finch, July 1964.

8. UM/RAO Instrumentation Memo No. 3, "Measurement of Noise Factor and Noise Temperature of Radio Astronomy Receivers for Space Vehicles", D. Walsh and B.G. Finch, 18 December 1962.

9. UM/RAO Technical Report No. 67-2, Instrumentation for Measurement of Cosmic Noise at 750, 1225, and 2000 kHz for a Rocket, W.J. Lindsay, et al., February 1967.

10. UM/RAO Technical Report No. 67-12, Cosmic Noise Intensity Measured from a Rocket, D. Walsh and F.T. Haddock, 7 December 1967.

11. UM/RAO Technical Report No. 71-1, Ground Support Equipment for the UM/RAO IMP-I Radio Astronomy Experiment, B.D. MacRae 31 January 1971.

12. UM/RAO Technical Report No. 67-3, Report on Development of Broad-band Noise Generator, B.G. Finch, February 1967.

TABLE 1.

RADIOMETER INPUT IMPEDANCE

Frequency	R_s	C_s
50 kHz	∞ ohms	3.5 picofarads
80	∞	3.5
130	∞	4.0
230	> 1 M	4.3
350	> 1 M	4.1
600	600 K	4.1
900	145 K	3.9
3530	13.7 K	2.1

R_s = Resistive component of preamplifier input impedance

C_s = Capacitive component of preamplifier input impedance

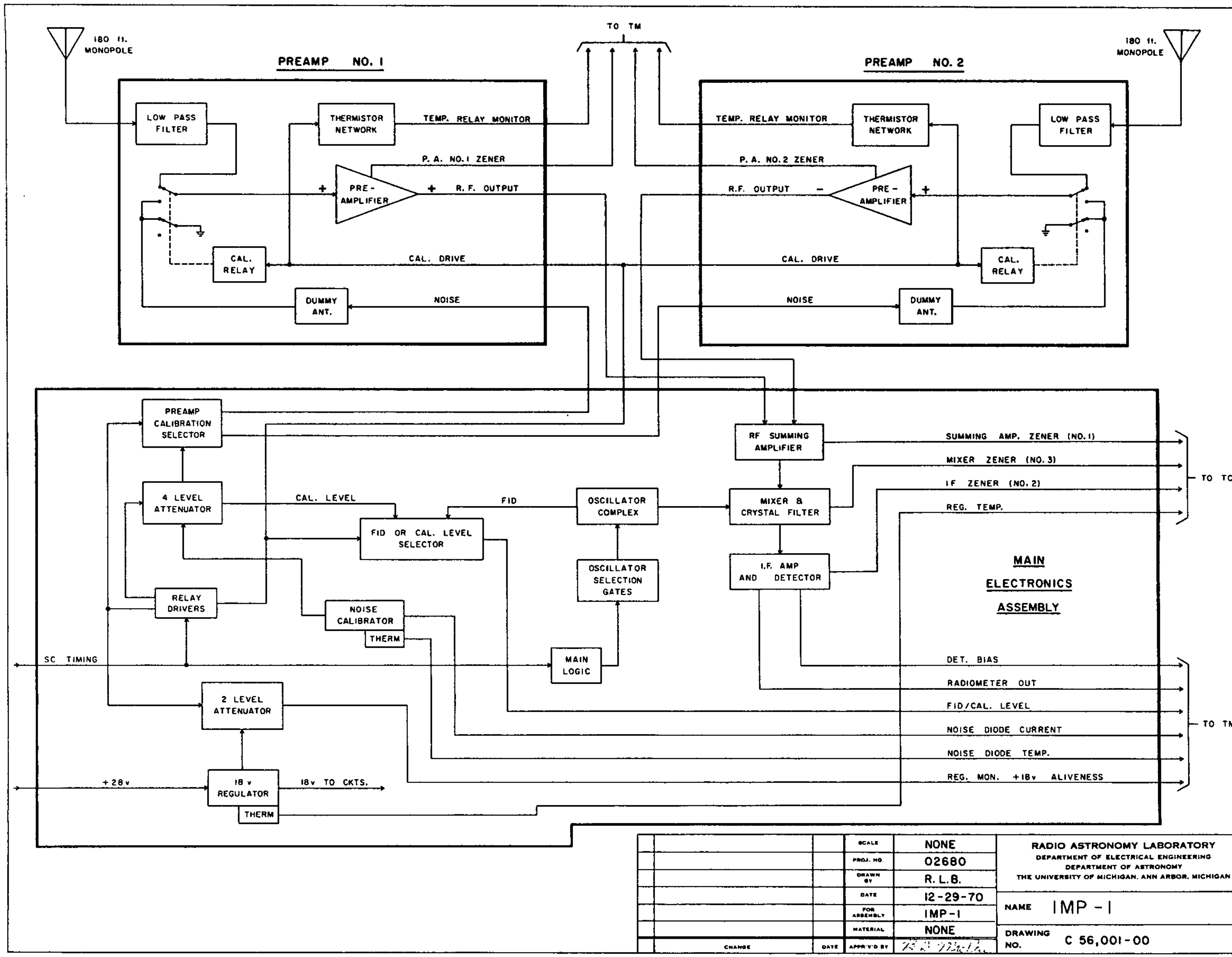

1. System Block Diagram

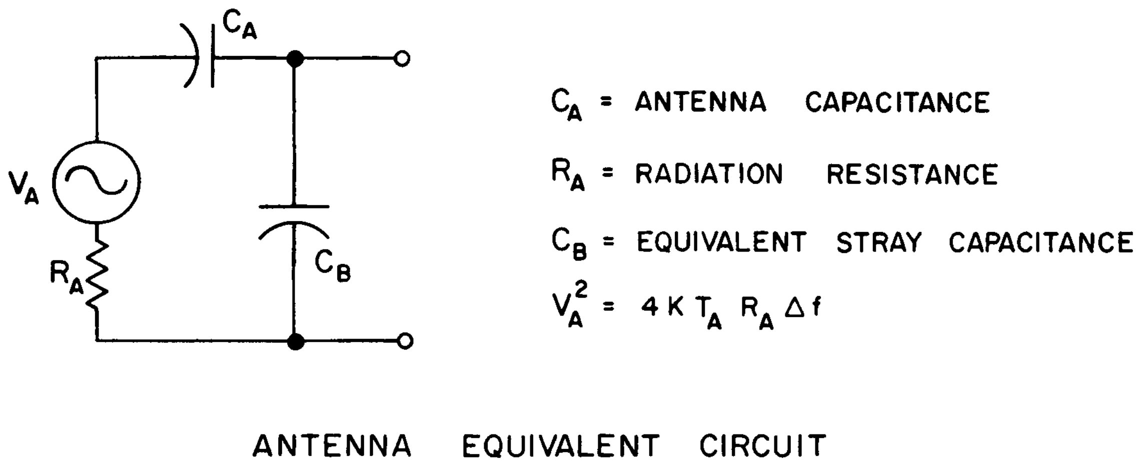

2. **Antenna Equivalent Circuit**

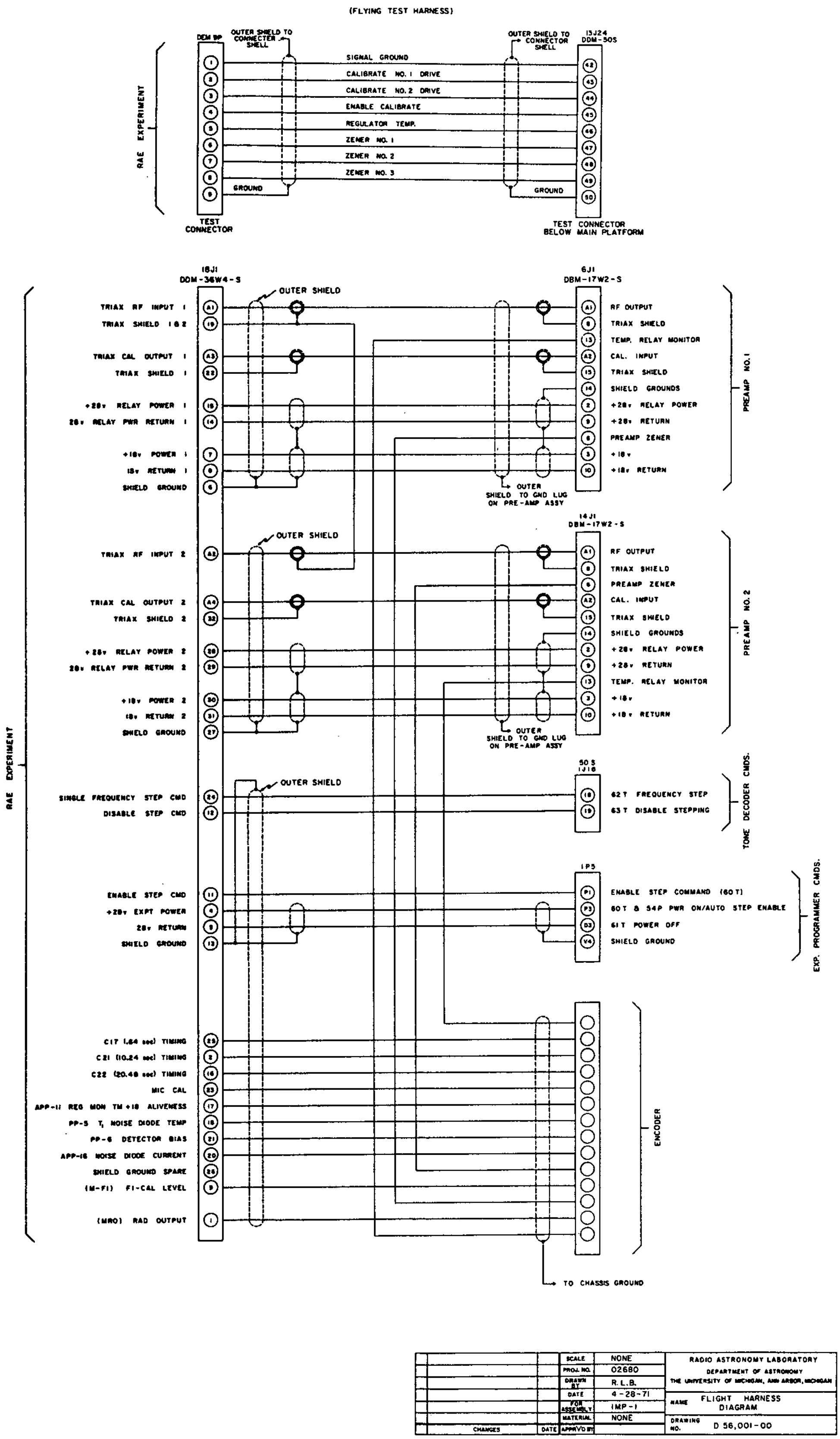

3. **Radiometer System Diagram**

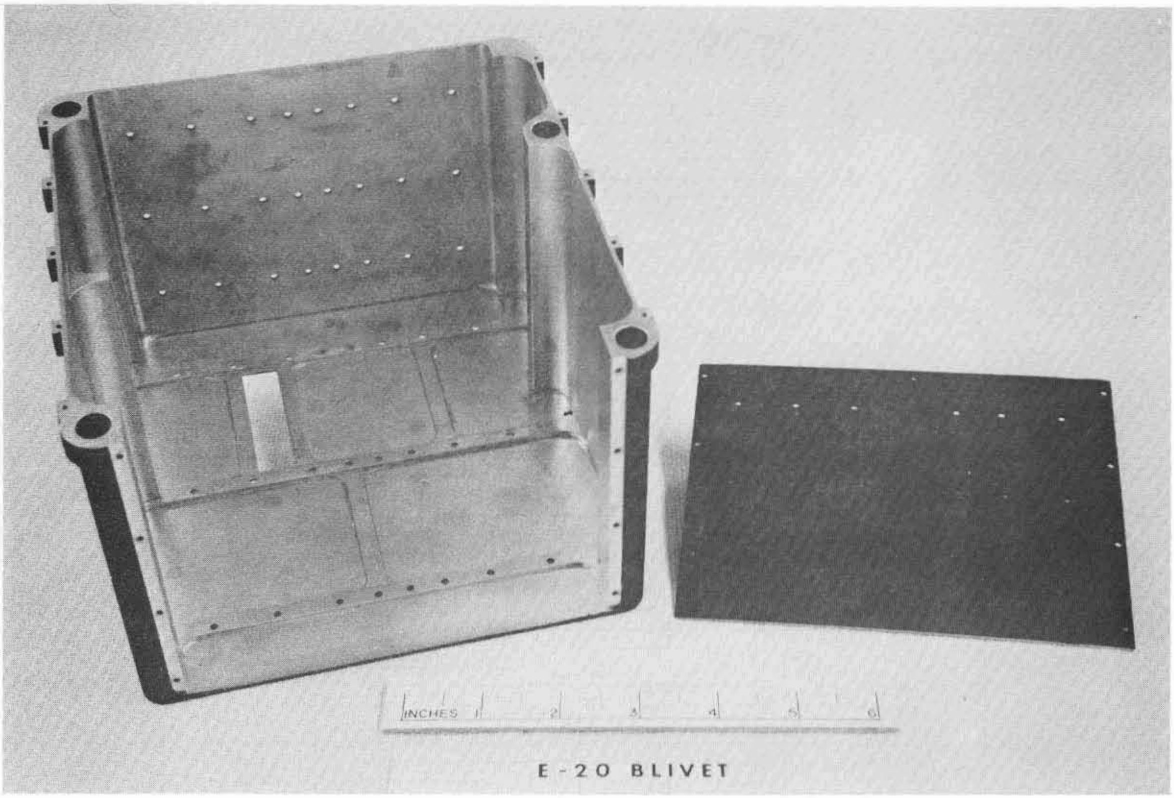

4. Main Electonics Package Blivet

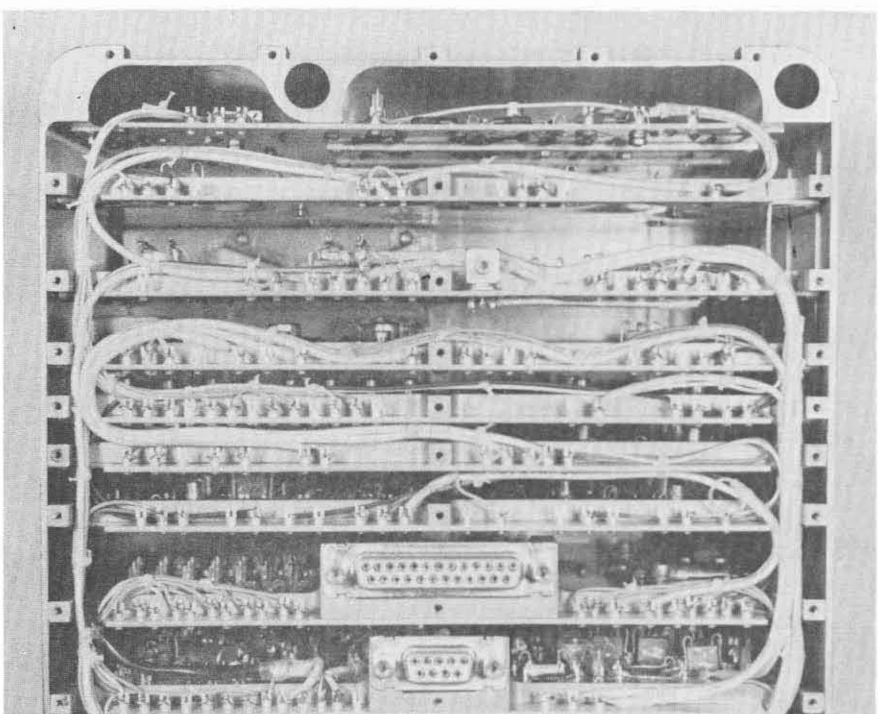

5. Assembled Main Electronics Package Without Cover

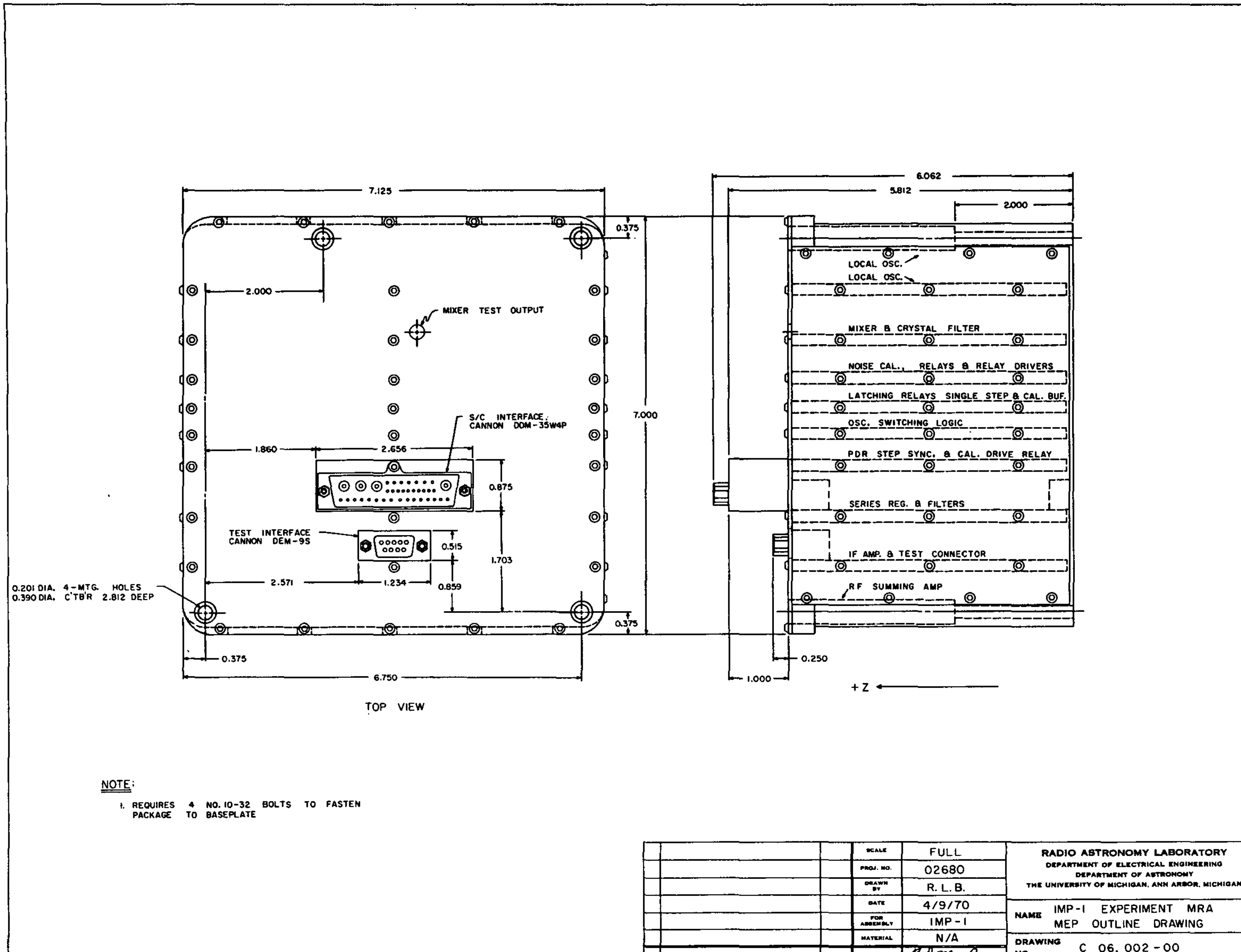

6. Main Electronics Package Mechanical Layout

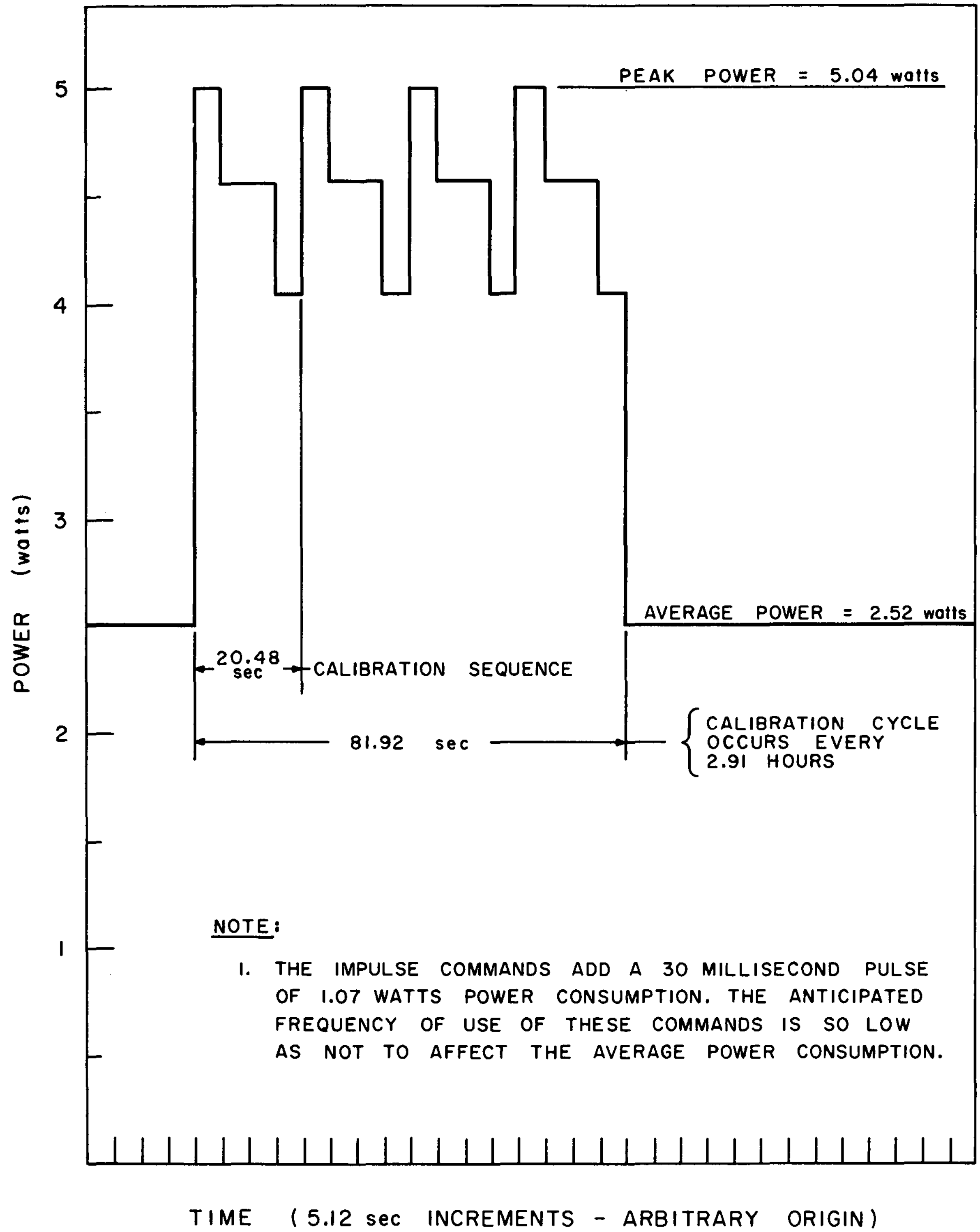

POWER PROFILE FOR IMP-1 RADIOMETER

7. Power Profile

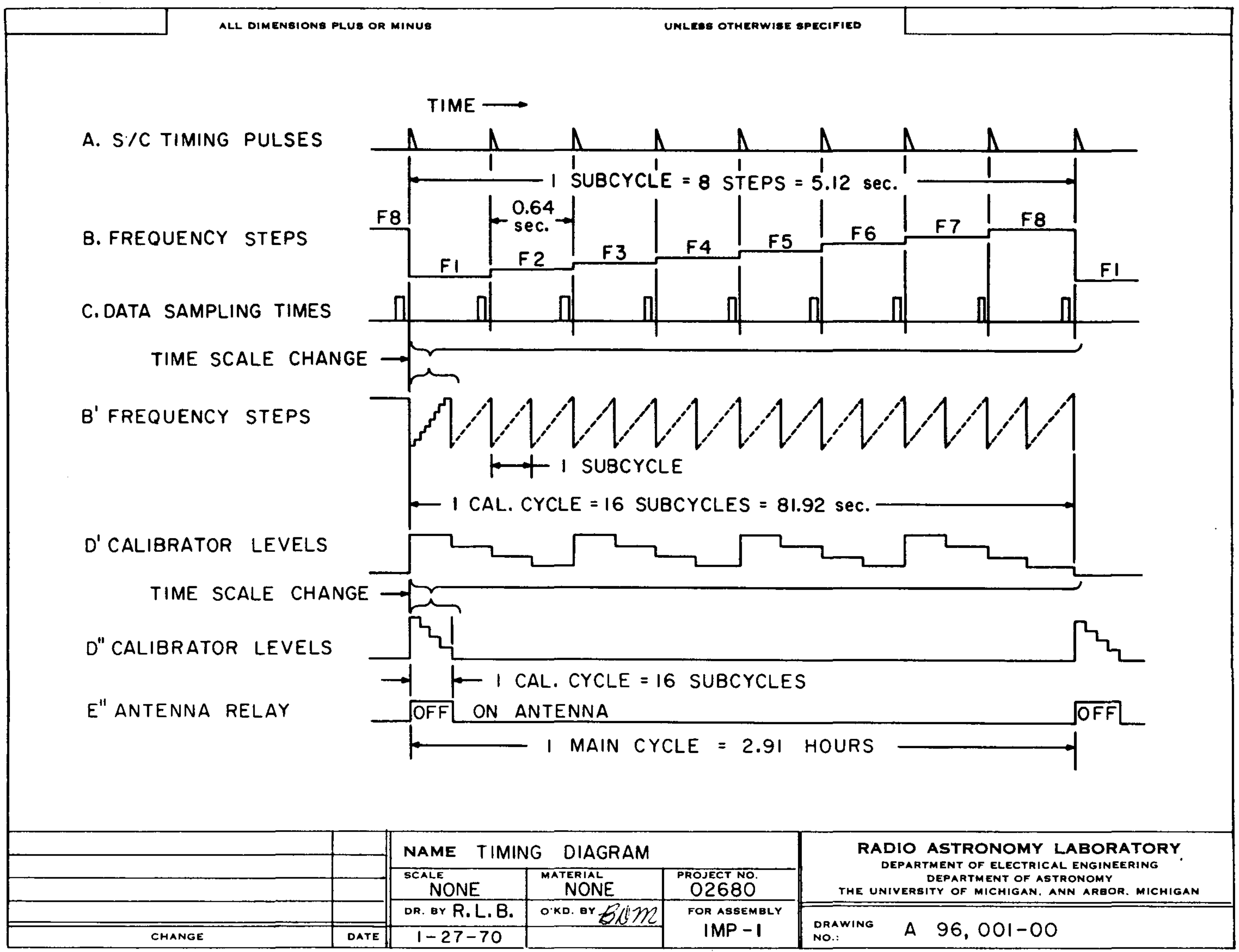

8. **Timing Sequence**

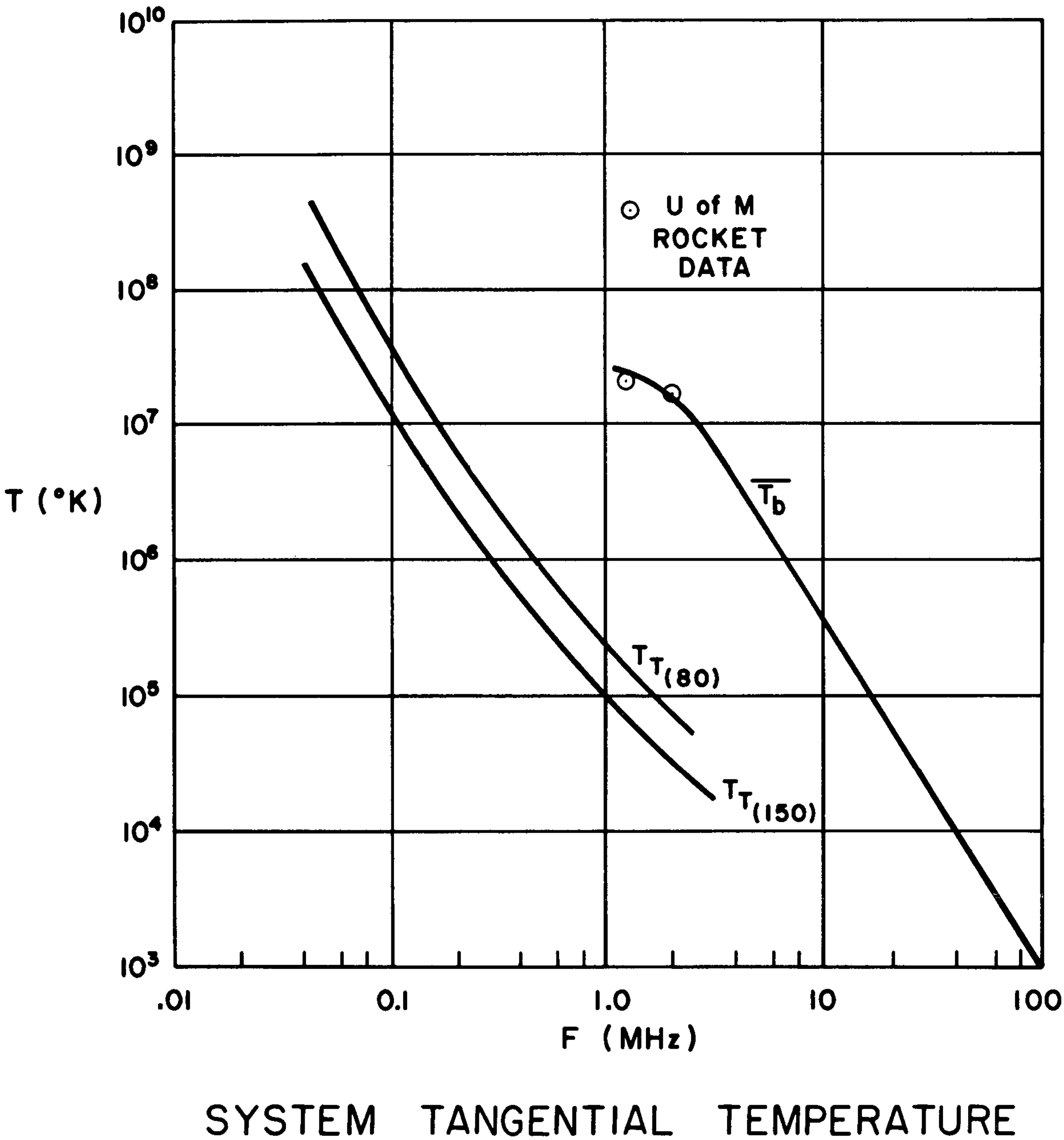

9. System Tangential Temperature

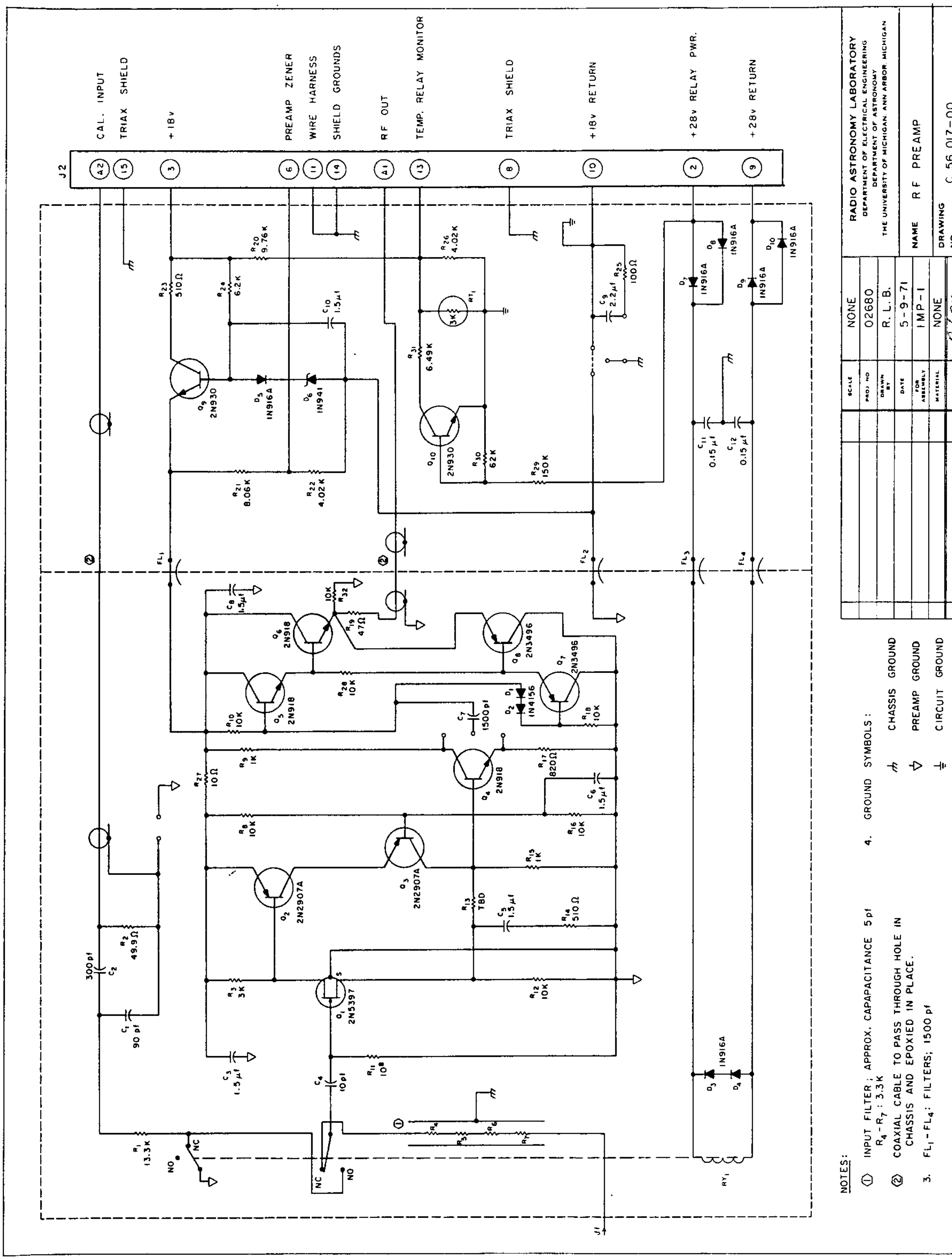

10. Preamplifier Circuit Diagram

(1)

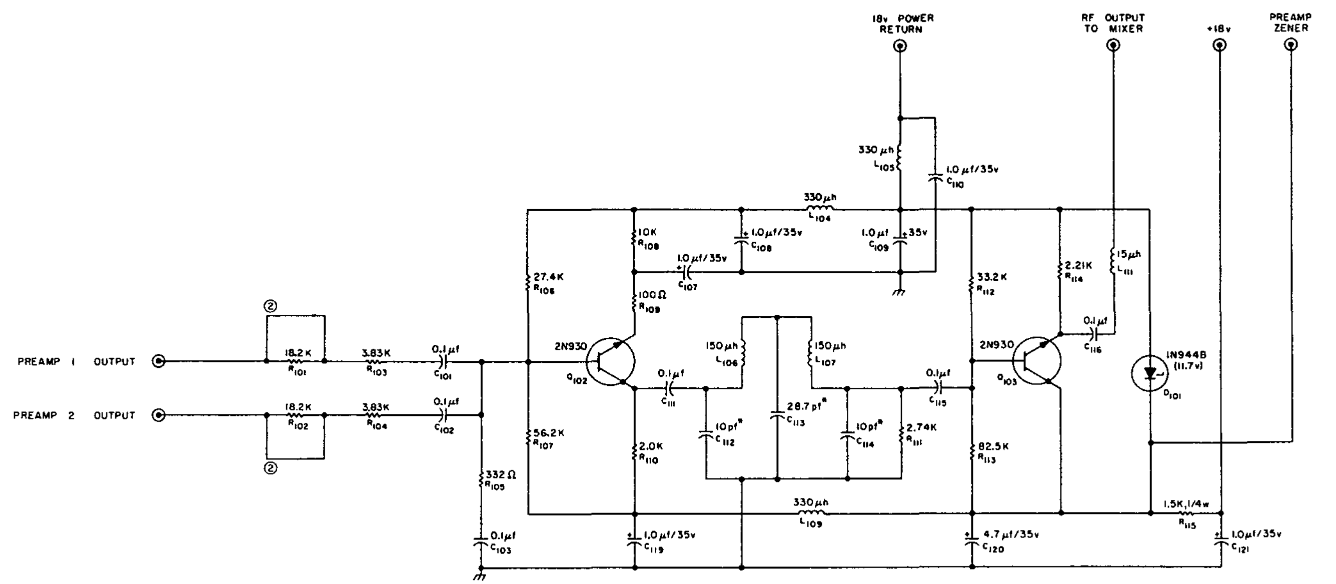

NOTES:

1. * INDICATES NOMINAL VALUES; ACTUAL CAPACITANCES WILL BE SELECTED.
2. CUTTABLE JUMPER

SCALE	NONE
PROJ NO	02680
DRAWN BY	R. L. B.
DATE	1-21-70
FOR ASSEMBLY	IMP-1
MATERIAL	NONE
APPR'V'D BY	BD M

CHANGE | DATE

RADIO ASTRONOMY LABORATORY
DEPARTMENT OF ELECTRICAL ENGINEERING
DEPARTMENT OF ASTRONOMY
THE UNIVERSITY OF MICHIGAN, ANN ARBOR, MICHIGAN

NAME RF SUMMING AMPLIFIER

DRAWING NO. C 56, 007-00

11. RF Summing Amplifier

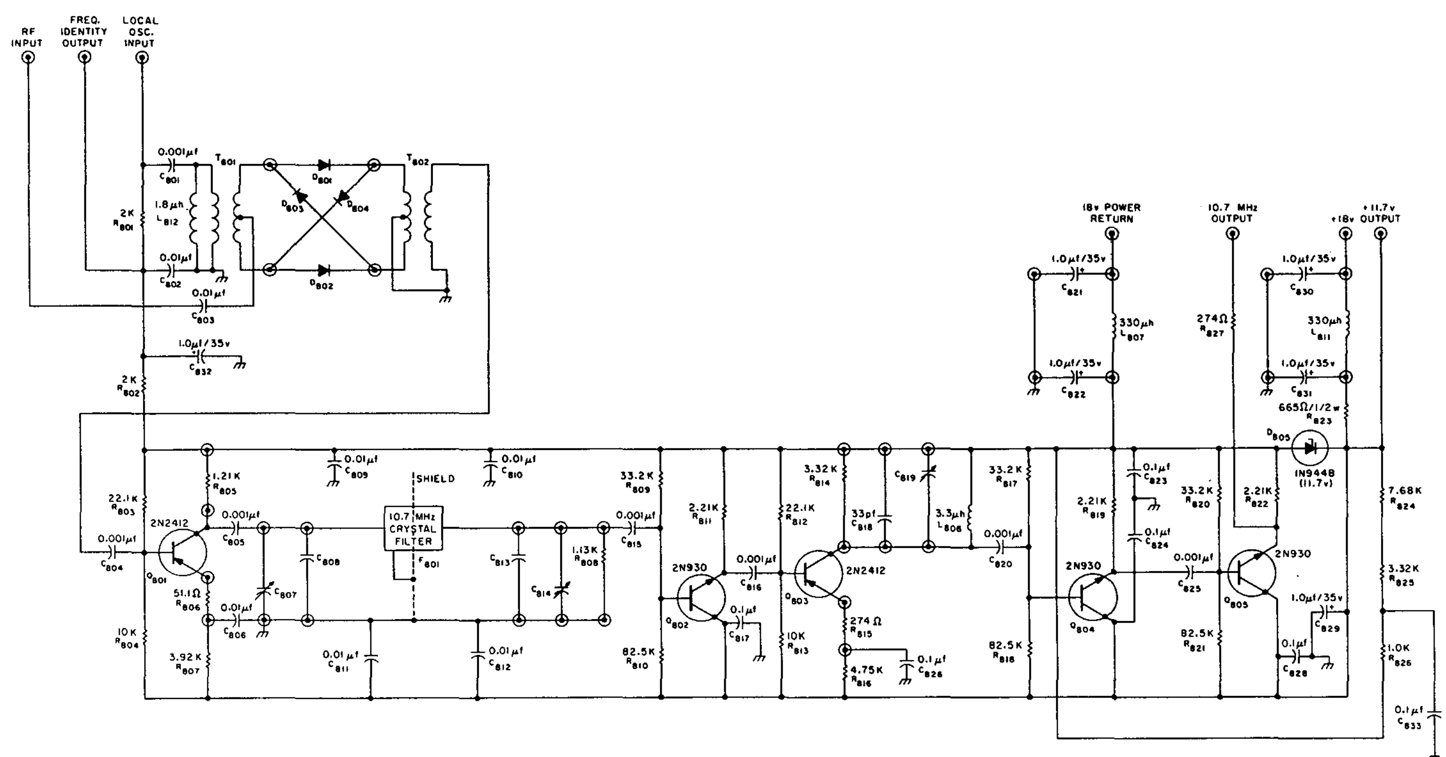

NOTE:

1. T_{801}, T_{802} ; 01-878-03 ALADDIN TRANSFORMER
2. C_{807}, C_{814}, C_{819} ; 5.5-18pf, 538-001-COPO-92P ERIE TRIMMERS
3. C_{808}, C_{813} ; SELECTED CAPACITORS (NOMINAL VALUE-15pf)
4. D_{801}-D_{802}, D_{803}-D_{804} ARE MATCHED PAIRS; IN498
5. C_{818} ; 301-N750 ERIE TEMPERATURE COMPENSATING CAPACITOR.
6. F_{801} ; MCOY R841

SCALE	NONE	RADIO ASTRONOMY LABORATORY DEPARTMENT OF ELECTRICAL ENGINEERING DEPARTMENT OF ASTRONOMY THE UNIVERSITY OF MICHIGAN, ANN ARBOR, MICHIGAN		
PROJ. NO.	02680			
DRAWN BY	R. L.B.			
DATE	8/11/70	NAME	MIXER, CRYSTAL FILTER, AND DRIVERS	
FOR ASSEMBLY	IMP-1			
MATERIAL	NONE	DRAWING NO.	C 56, 010-00	
APPR'V'D BY	B L M			

CHANGE | DATE

12. Mixer, Crystal Filter, and Drivers

2 (4)

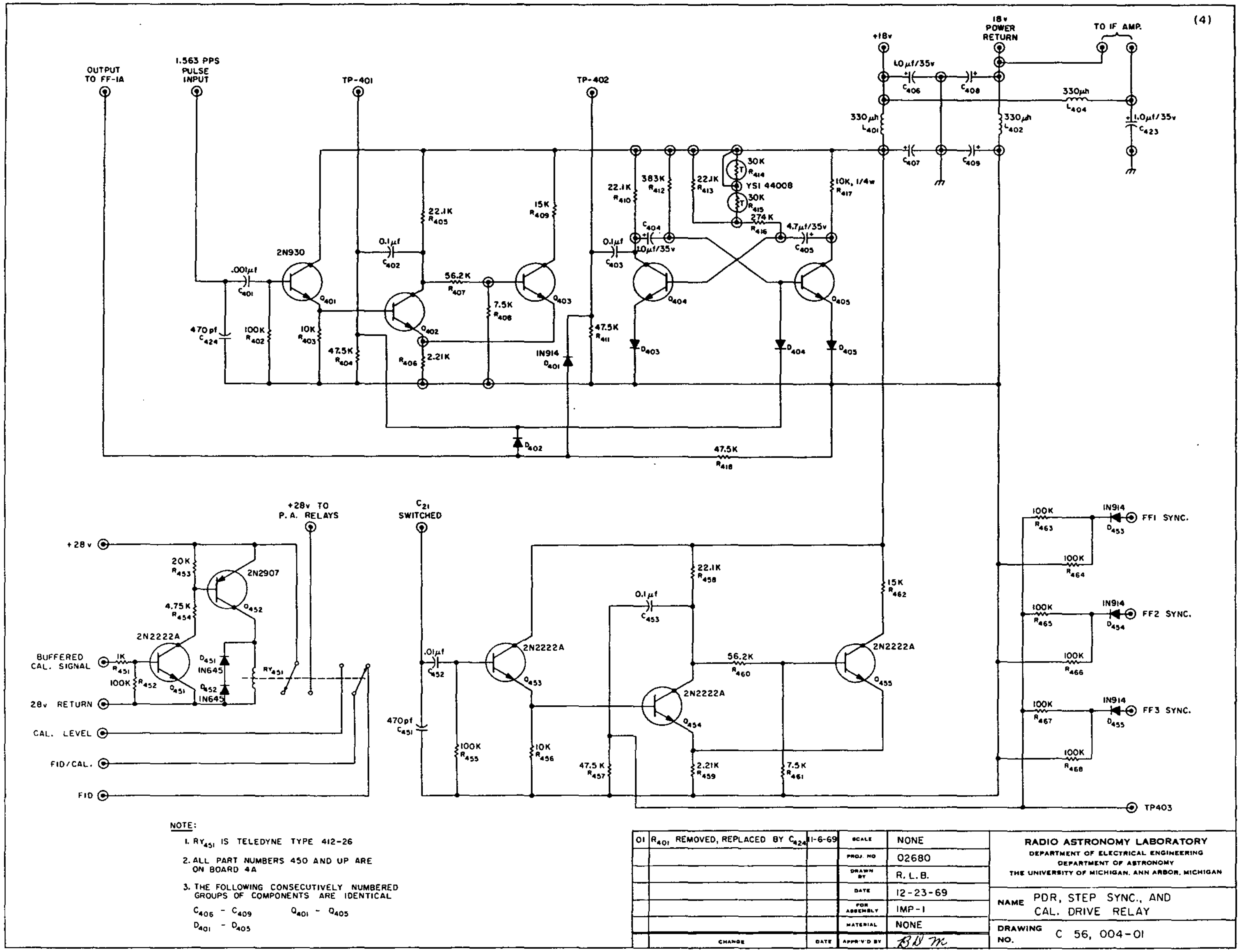

13. PDR, Stepping Synchronizer, and Calibration Drive Relays

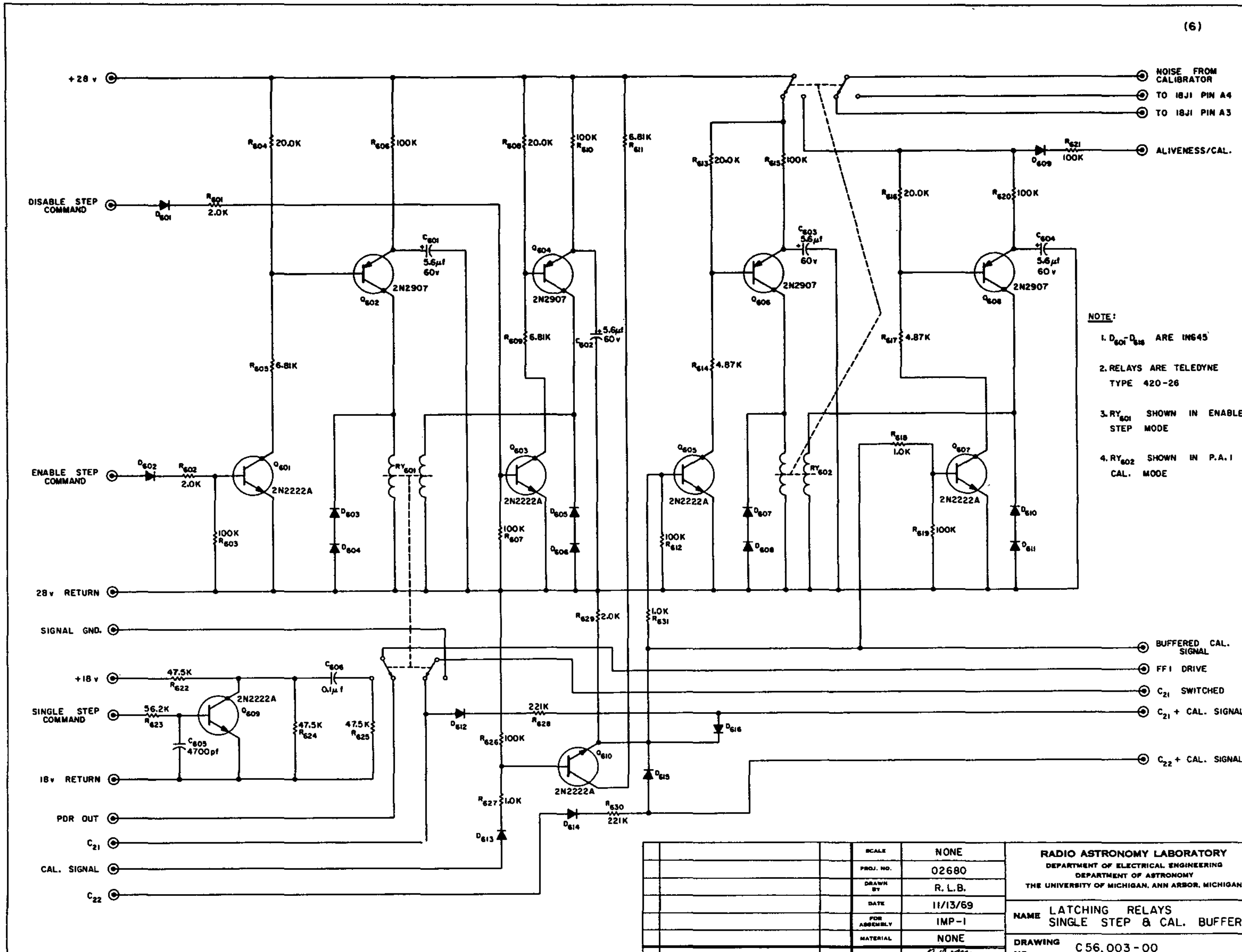

14. Single Step and Calibration Control Circuitry

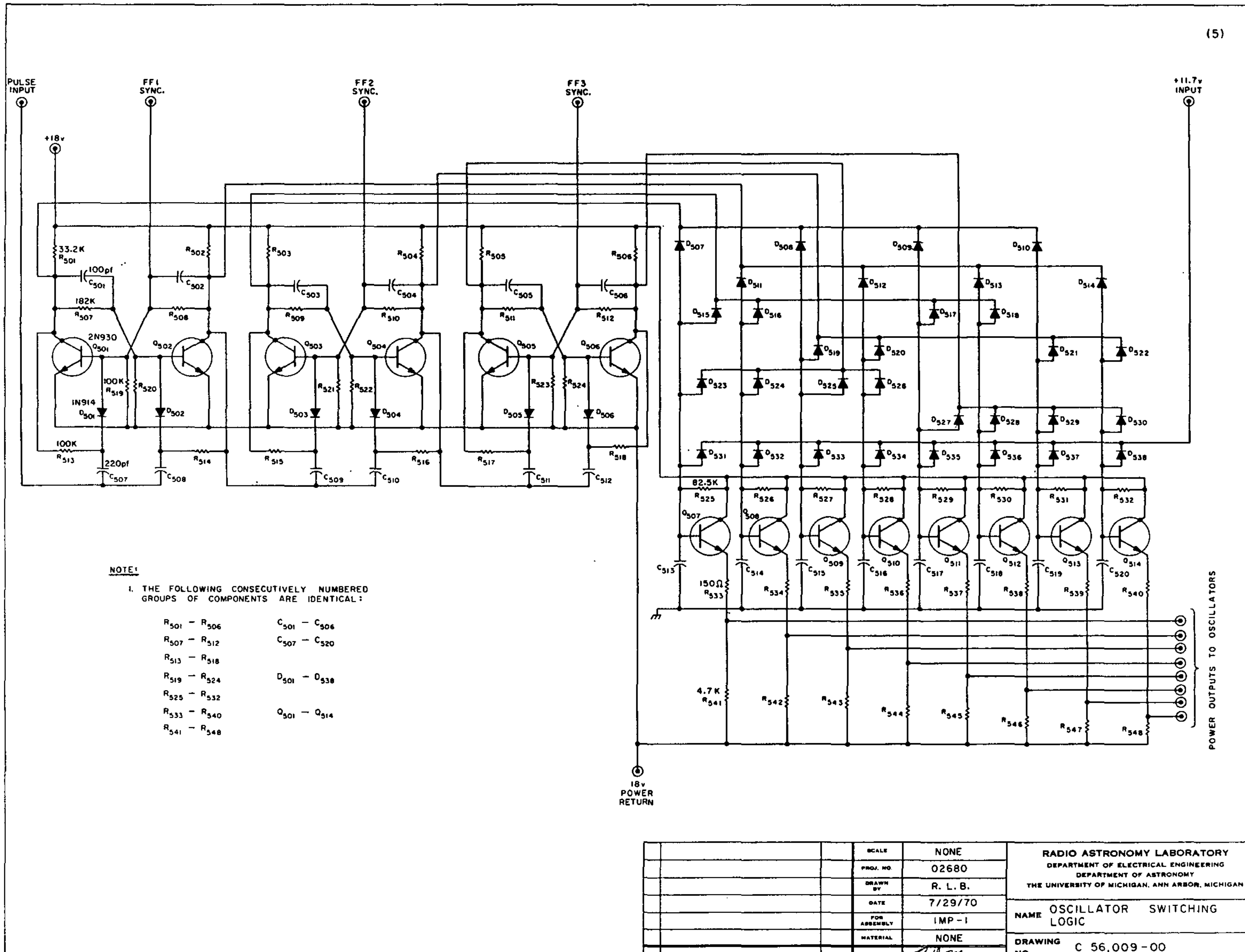

15. Oscillator Switching Logic

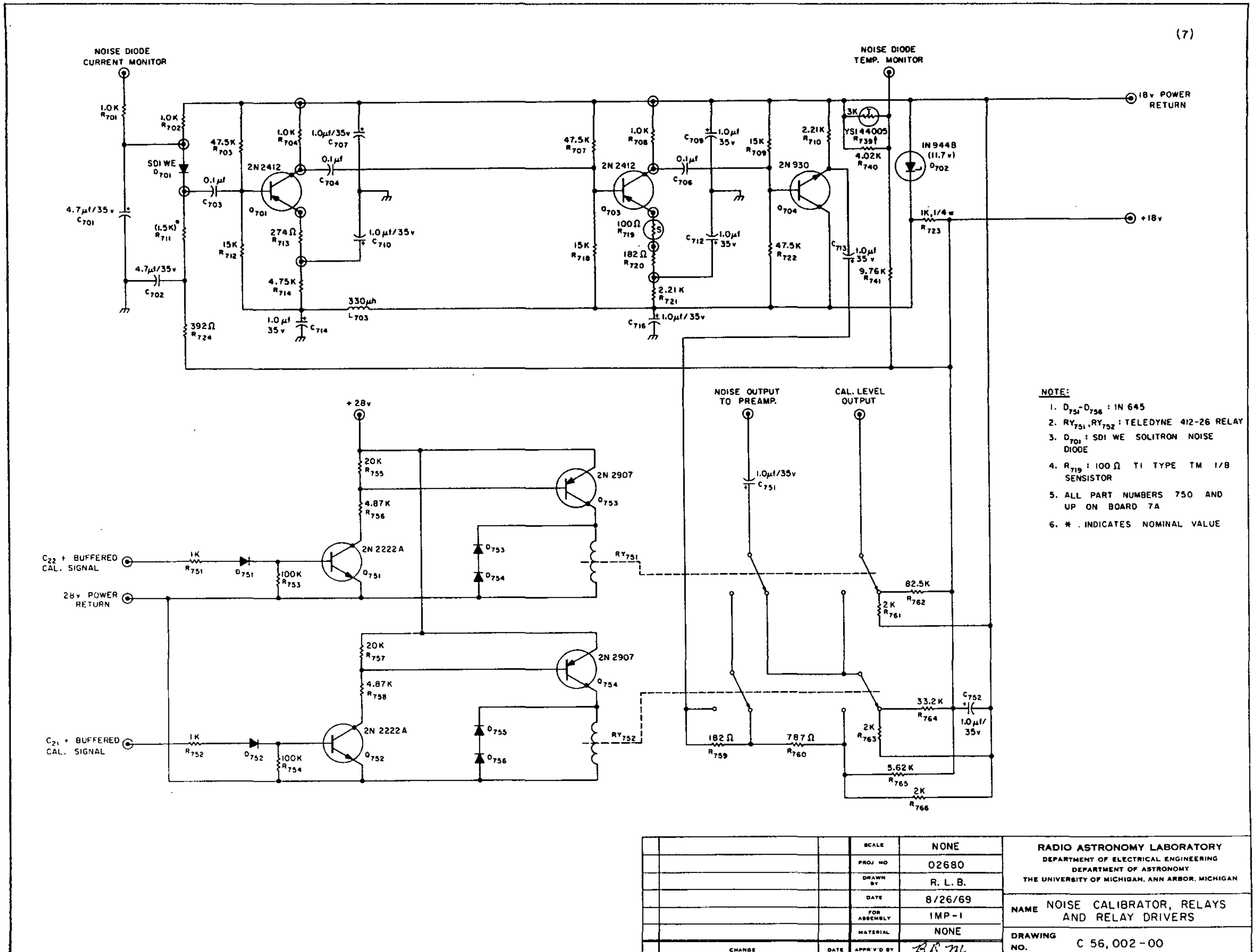

16. Noise Calibration Circuitry

(9 & 10)

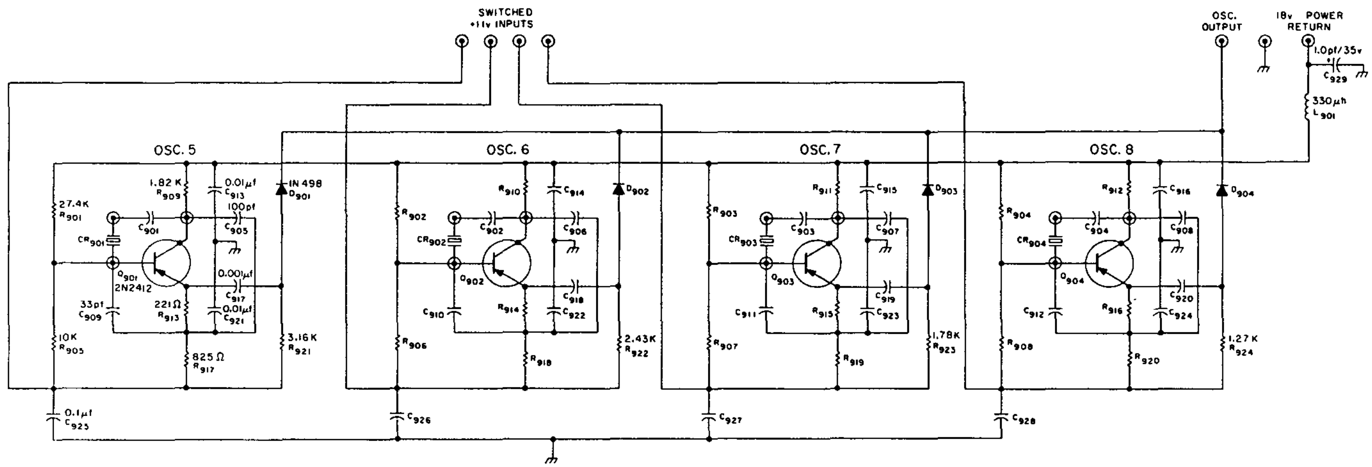

NOTE:

1. THE FOLLOWING CONSECUTIVELY NUMBERED GROUPS OF COMPONENTS ARE IDENTICAL:

$R_{901} - R_{904}$	$C_{905} - C_{908}$	$Q_{901} - Q_{904}$
$R_{905} - R_{908}$	$C_{909} - C_{912}$	
$R_{909} - R_{912}$	$C_{913} - C_{916}$	$D_{901} - D_{904}$
$R_{913} - R_{916}$	$C_{917} - C_{920}$	
$R_{917} - R_{920}$	$C_{921} - C_{924}$	
	$C_{925} - C_{928}$	

2. $C_{901} - C_{904}$, SELECTED CAPACITORS (FINAL SELECTED VALUE 47pf)

3. CIRCUIT BOARDS 9 AND 10 ARE IDENTICAL WITH THE FOLLOWING EXCEPTIONS:
   A. THE FILTER (L_{901} & C_{929}) OCCURS ON BOARD 9 ONLY AND IS USED BY BOTH BOARDS.
   B. BOARD 10 CONTAINS OSCILLATORS 1-4
   C. COMPONENT NUMBERS ARE IN 1000 SERIES.
   D. R_{1021} - 9.76K
      R_{1022} - 7.15K
      R_{1023} - 5.49K
      R_{1024} - 4.12K
      R_{1009} - 1.5 K

CHANGE	DATE		
		SCALE	NONE
		PROJ NO	02680
		DRAWN BY	R. L. B.
		DATE	9-14-70
		FOR ASSEMBLY	IMP-1
		MATERIAL	NONE
		APPR'V'D BY	[illegible]

RADIO ASTRONOMY LABORATORY
DEPARTMENT OF ELECTRICAL ENGINEERING
DEPARTMENT OF ASTRONOMY
THE UNIVERSITY OF MICHIGAN ANN ARBOR, MICHIGAN

NAME LOCAL OSCILLATORS

DRAWING NO. C 56,011-00

17. Local Oscillators

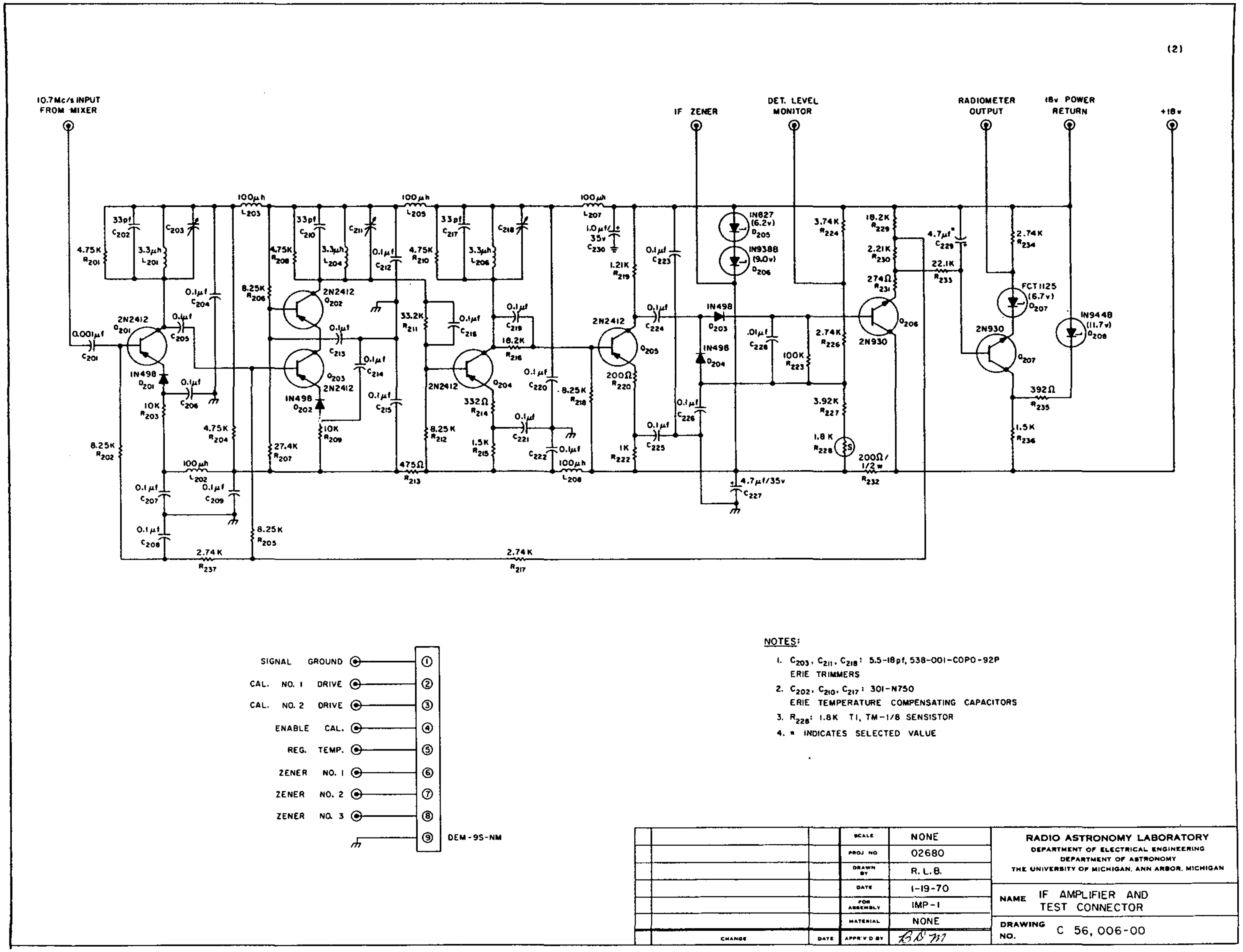

18. IF Amplifier and Detector

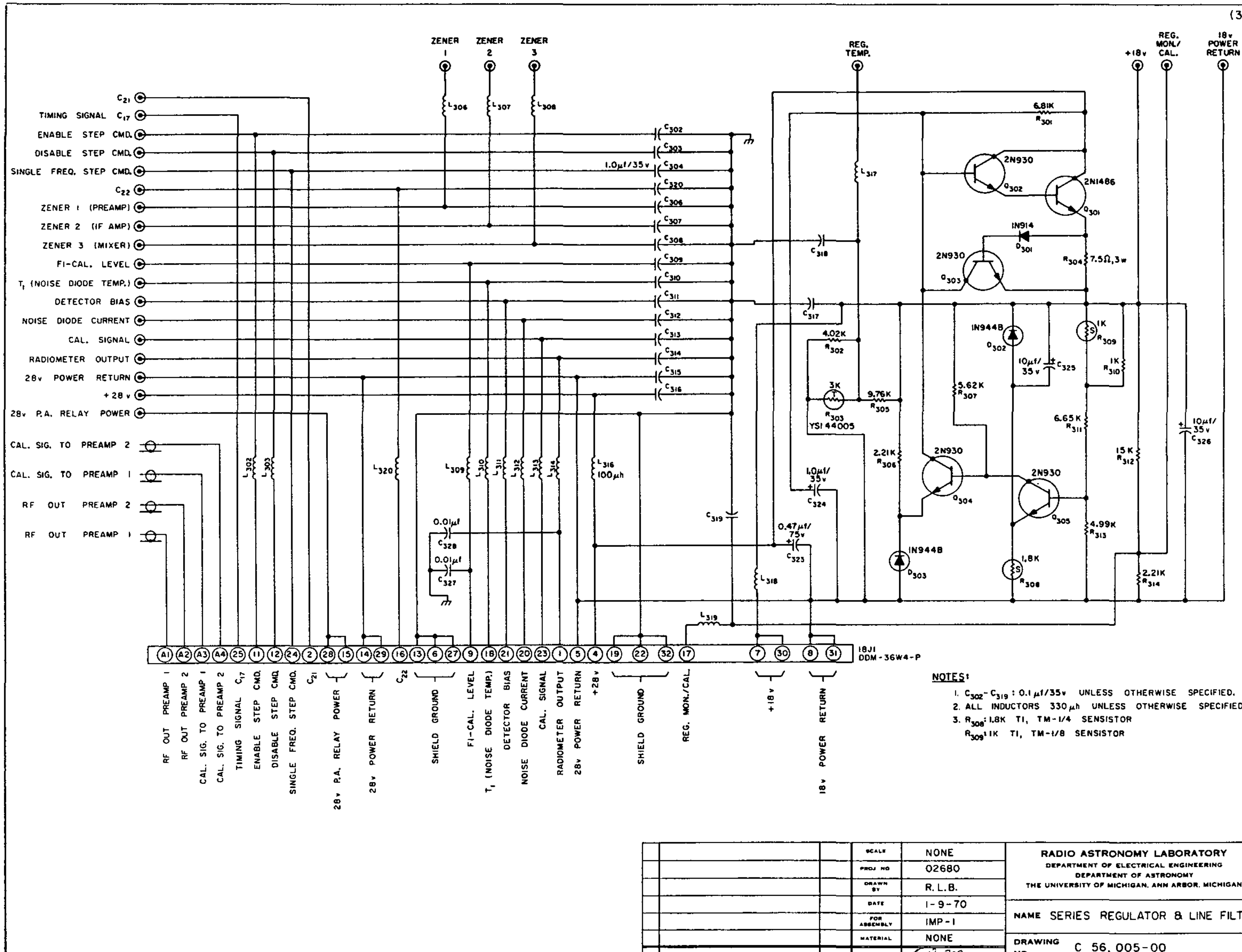

19. Series Regulator and Line Filters

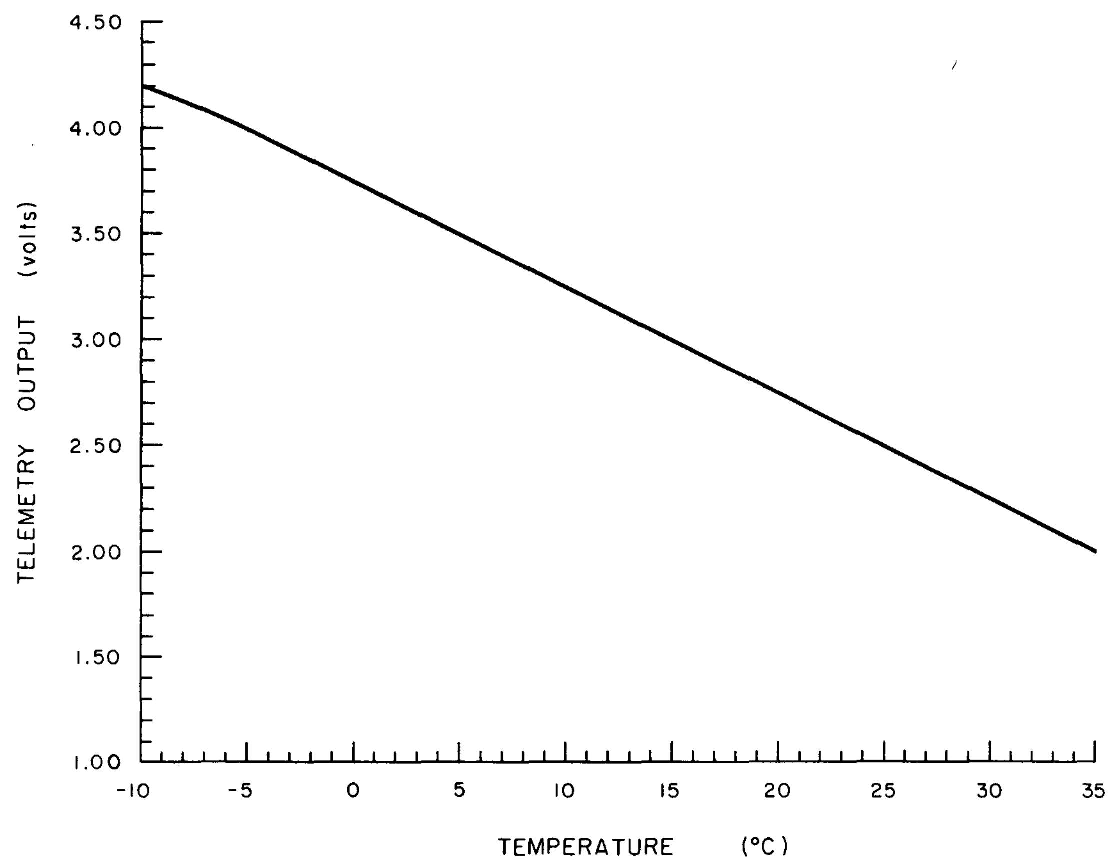

IMP-I PREAMP AND NOISE DIODE THERMISTOR CALIBRATION

20. Thermistor Calibration Curve

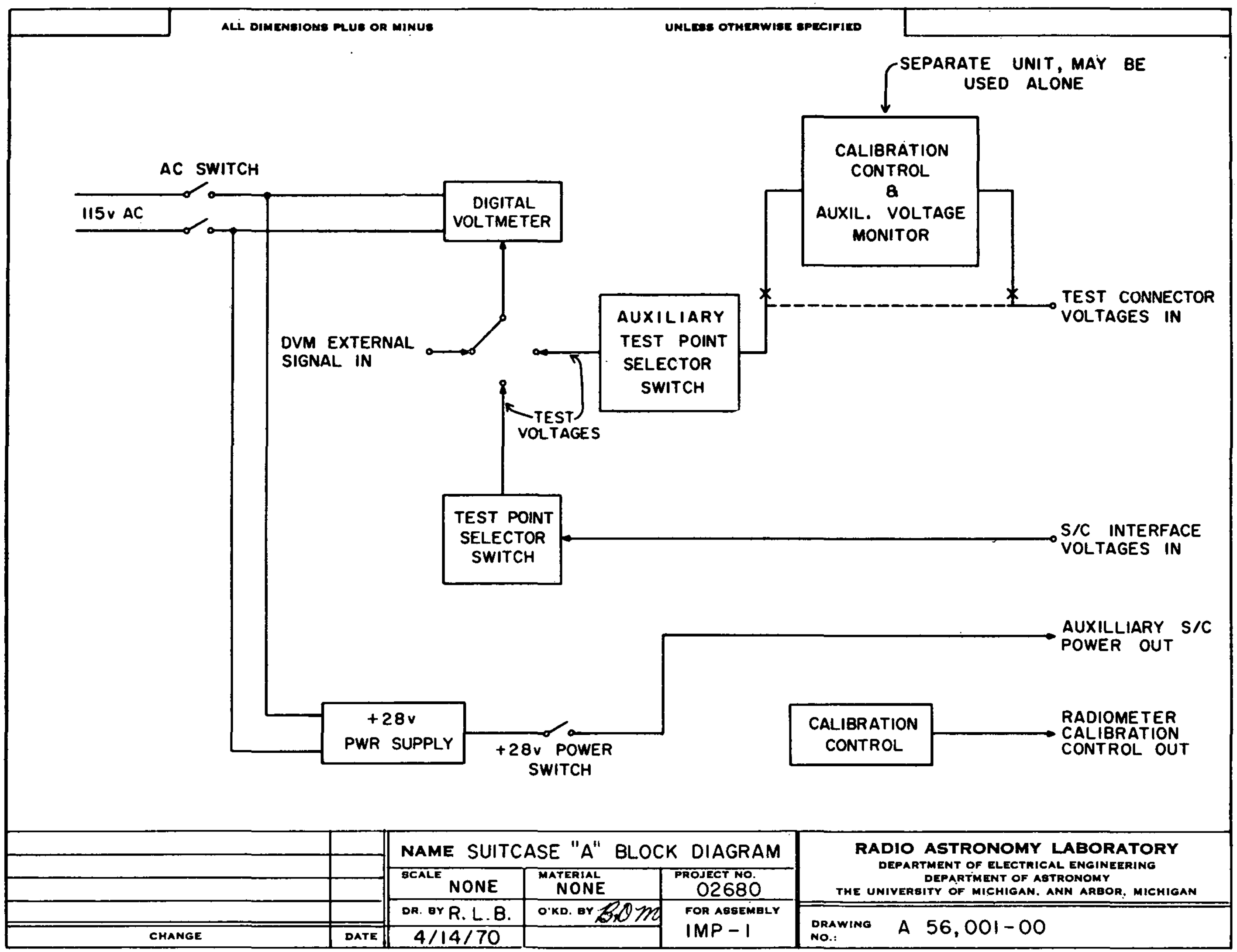

21. Suitcase "A" Block Diagram

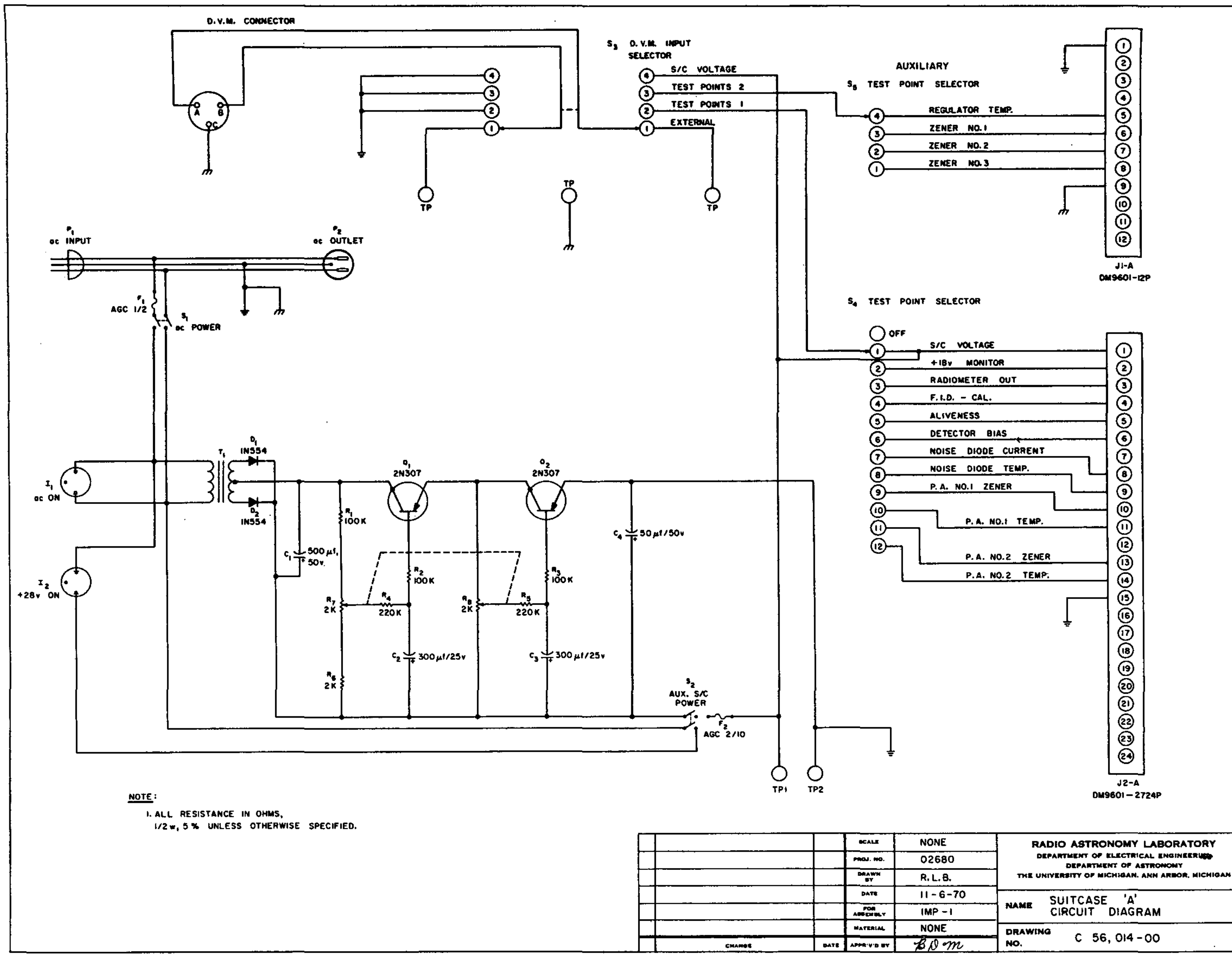

22. Suitcase "A" Circuit Diagram

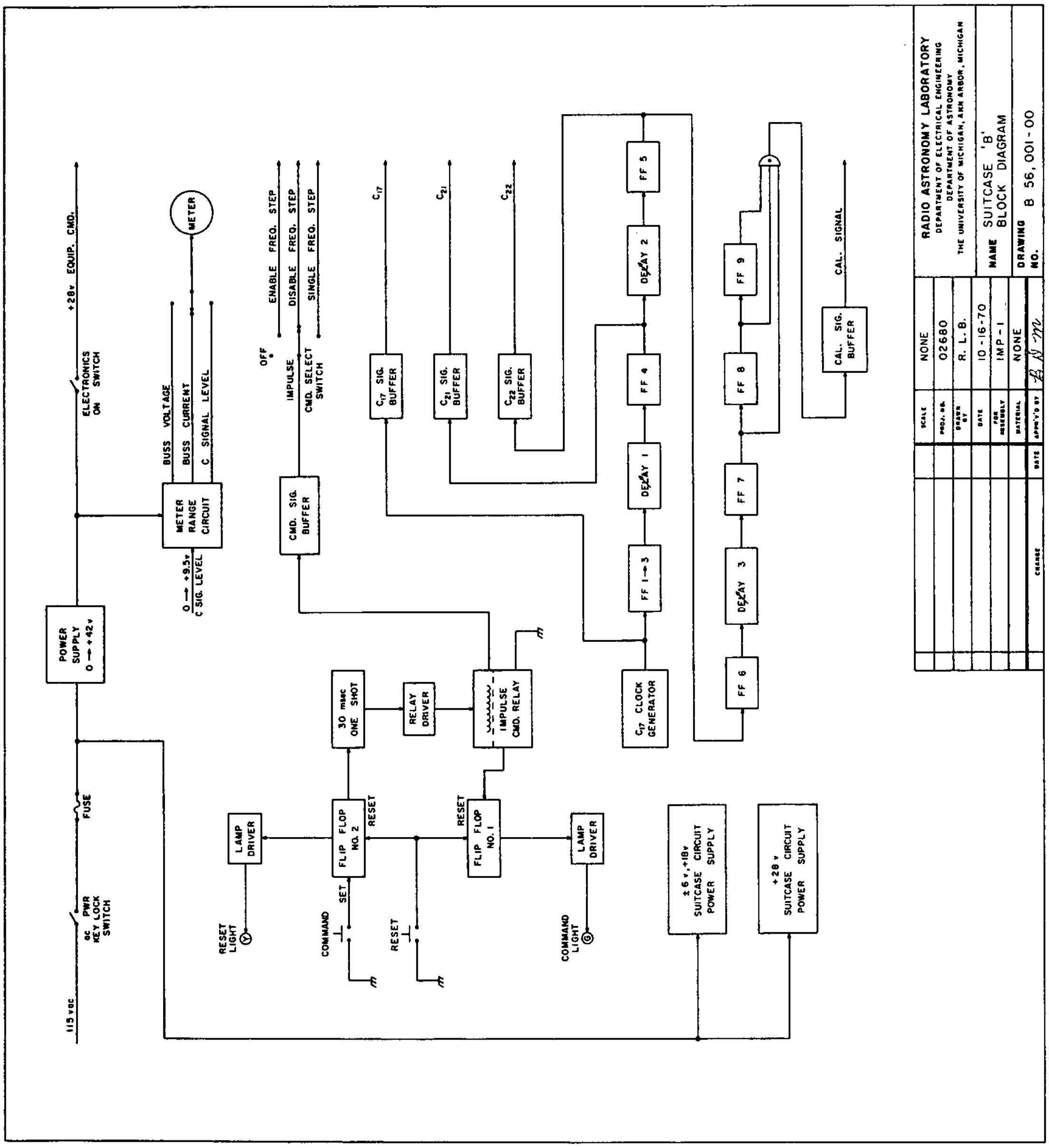

23. Suitcase "B" Block Diagram

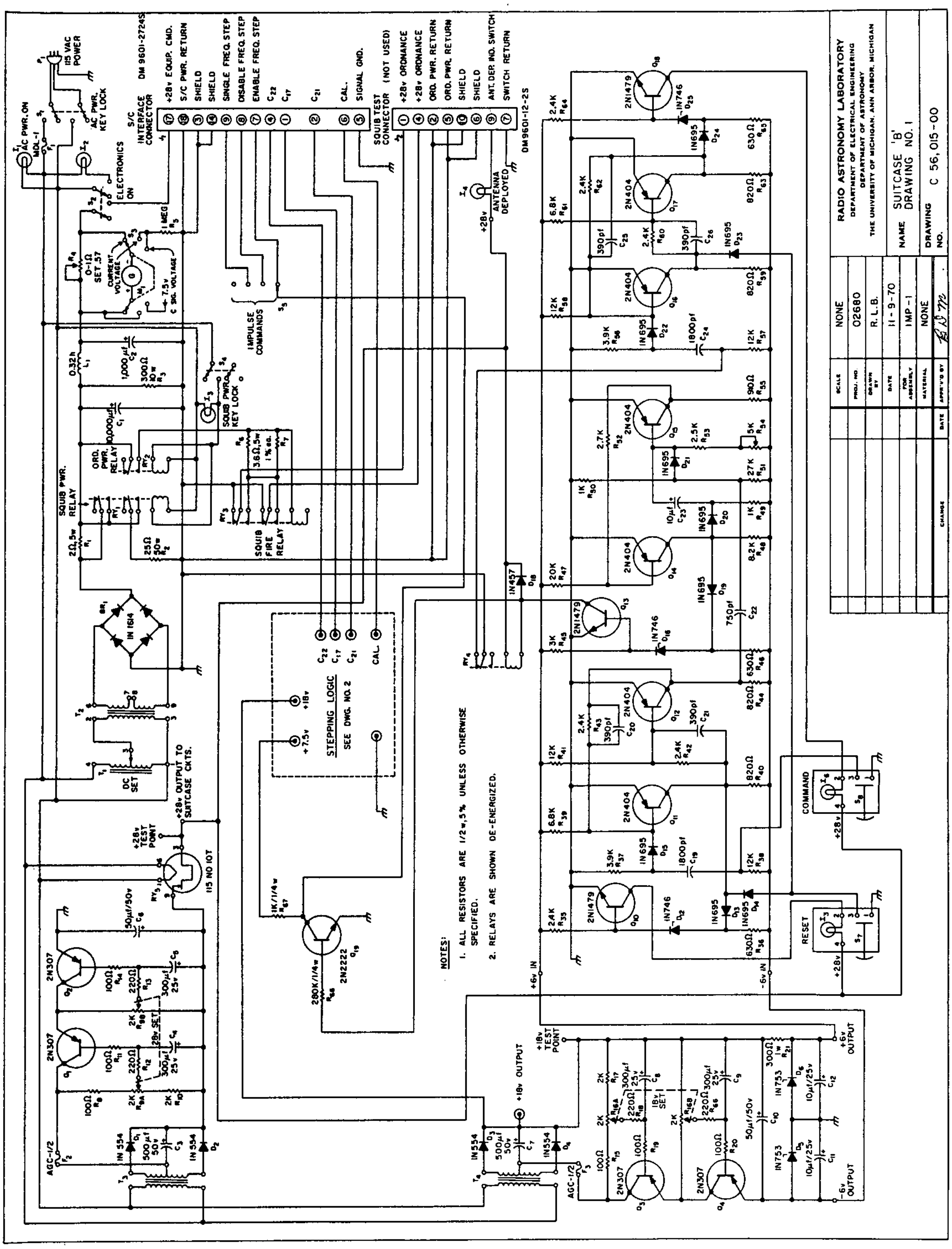

24. Suitcase "B" Circuit Diagram

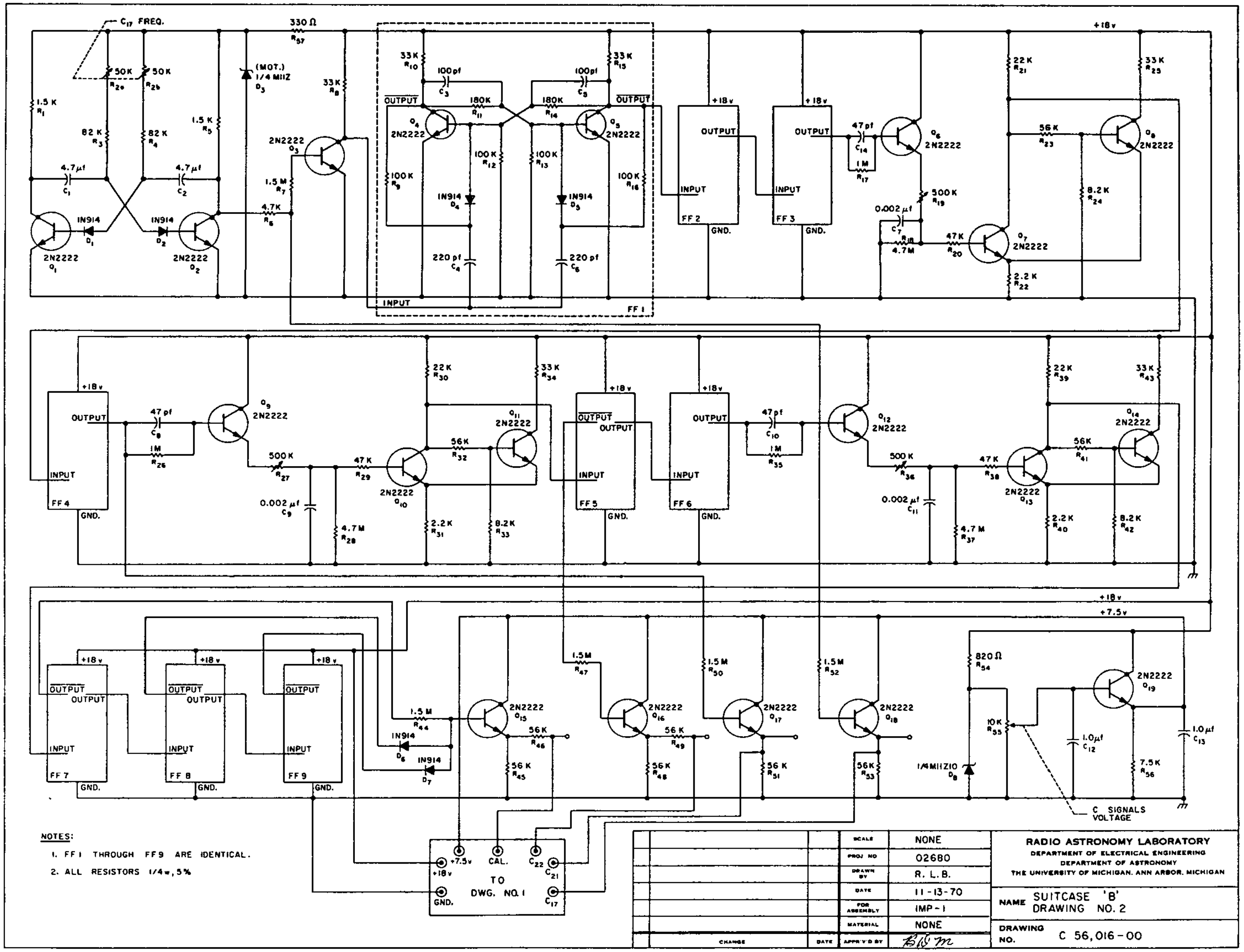

25. Suitcase "B" Circuit Diagram

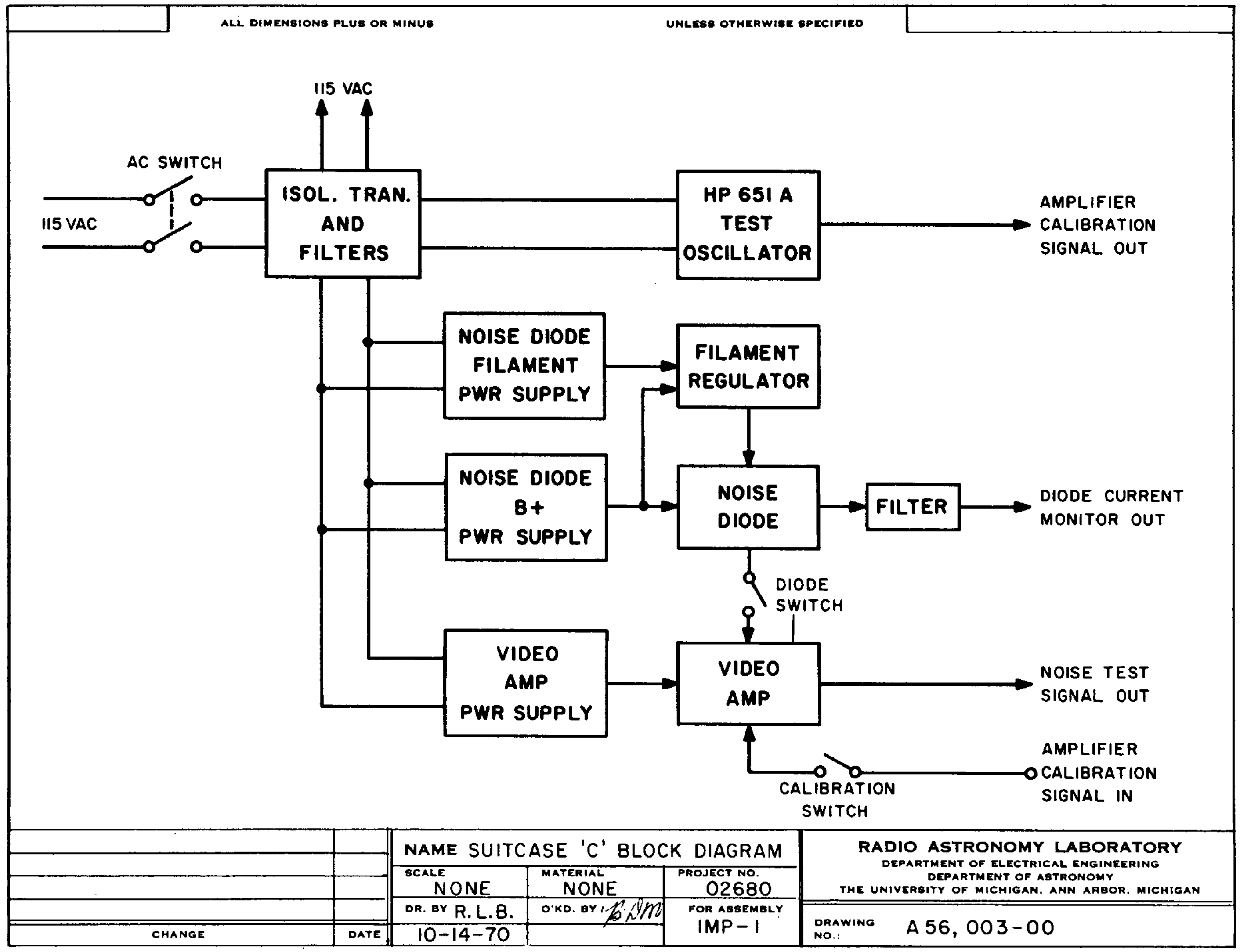

26. Suitcase "C" Block Diagram

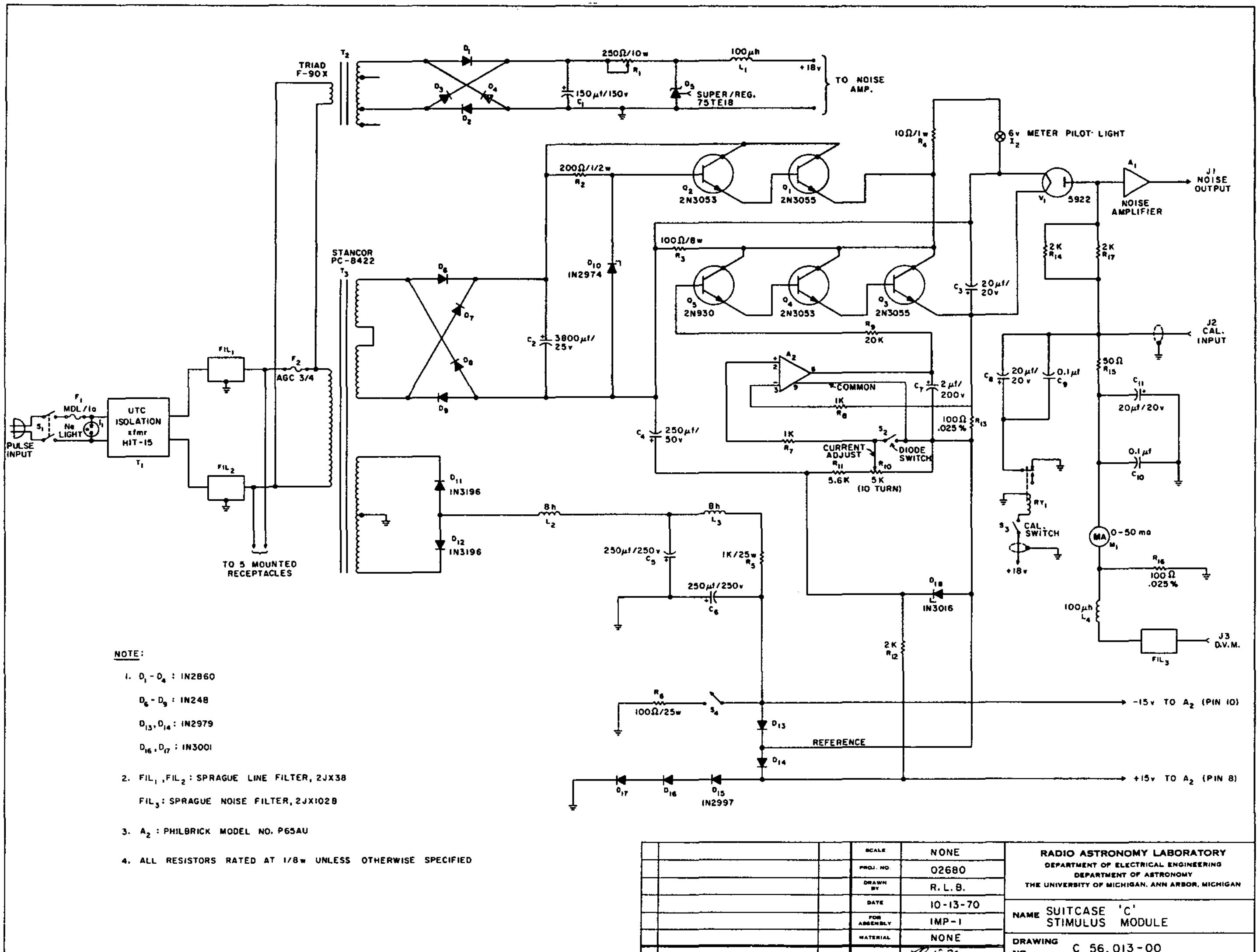

27. Suitcase "C" Circuit Diagram

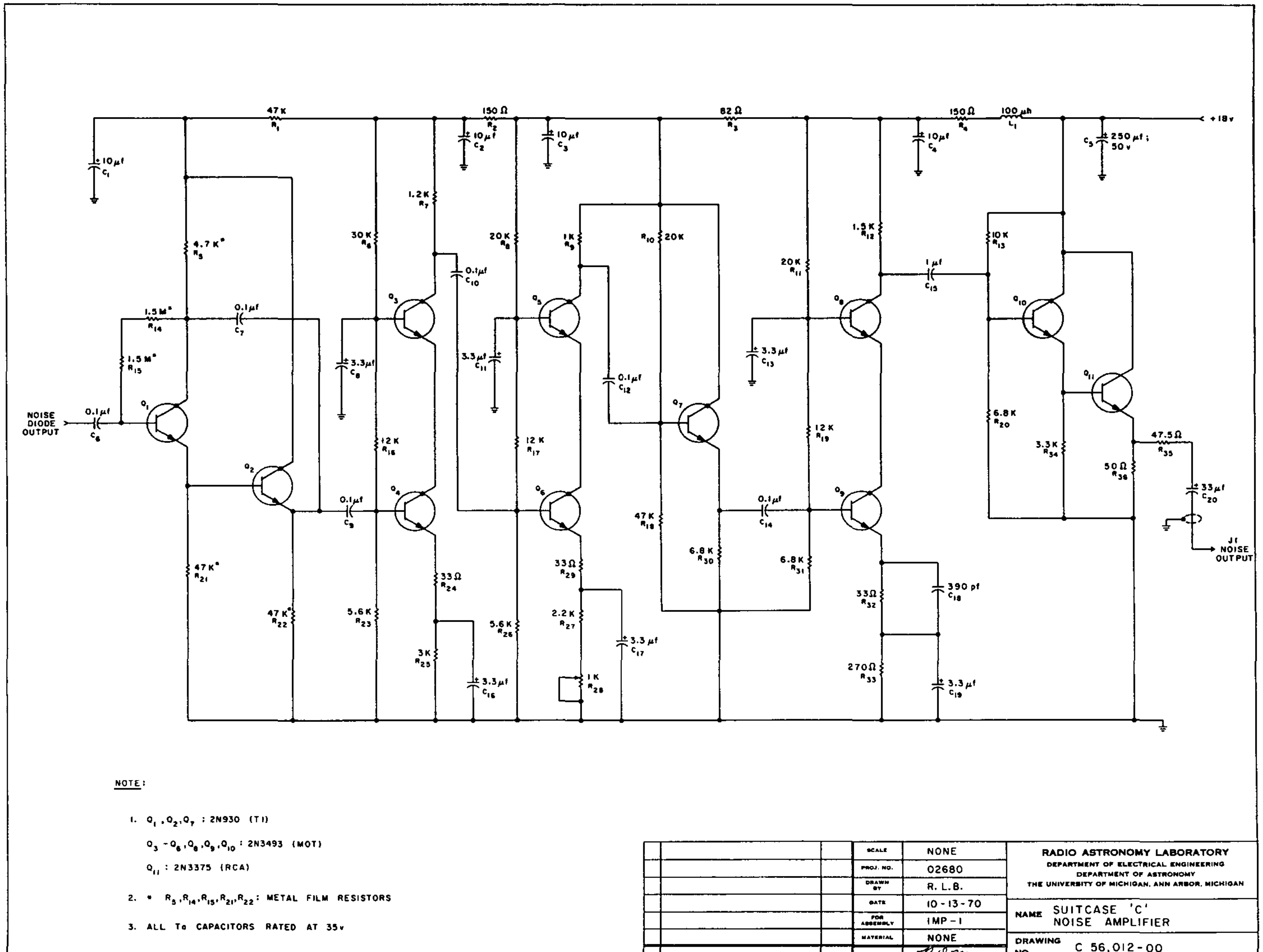

28. Suitcase "C" Noise Amplifier Circuit Diagram

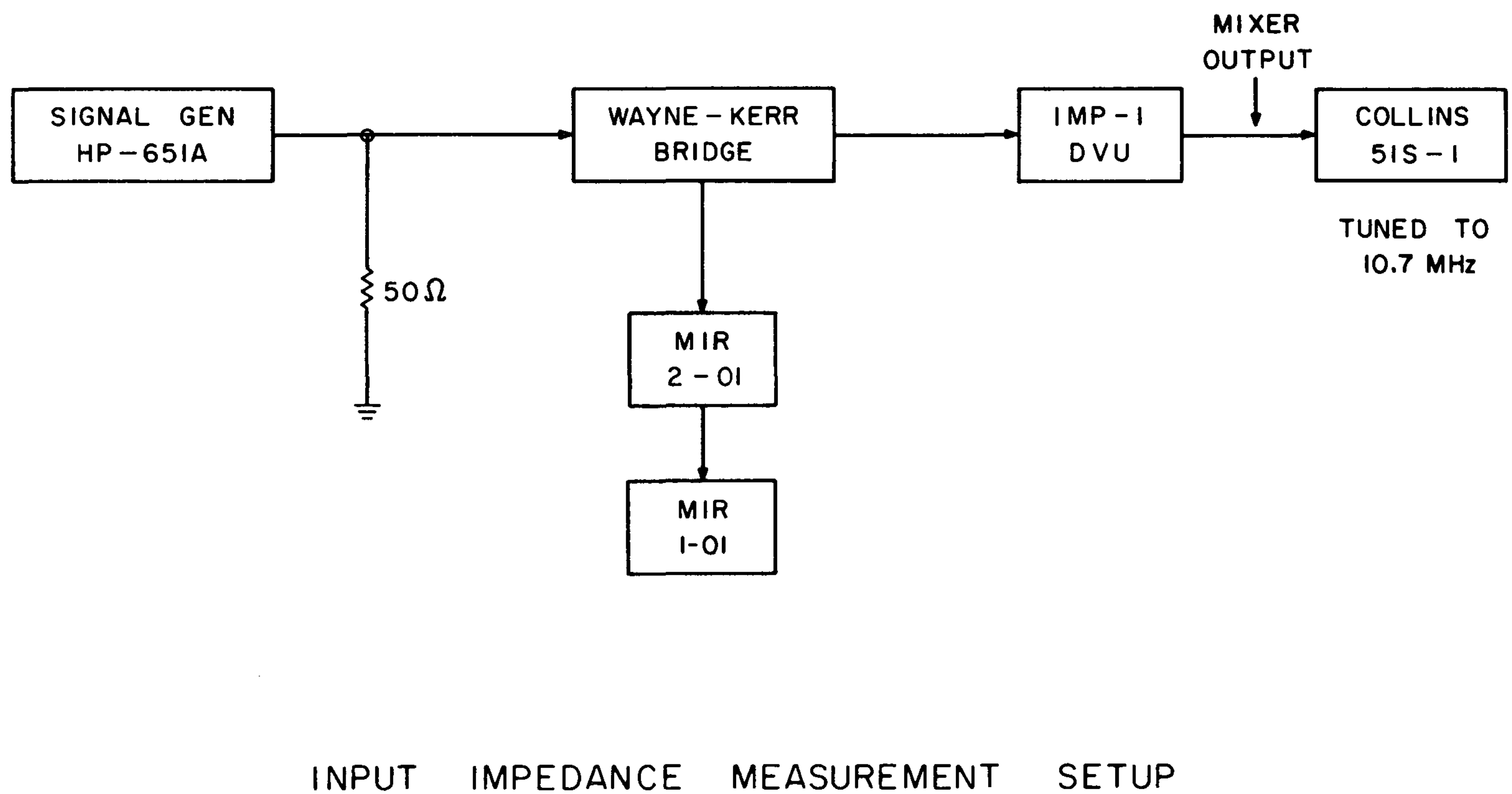

29. **Input Impedance Measurement Setup**

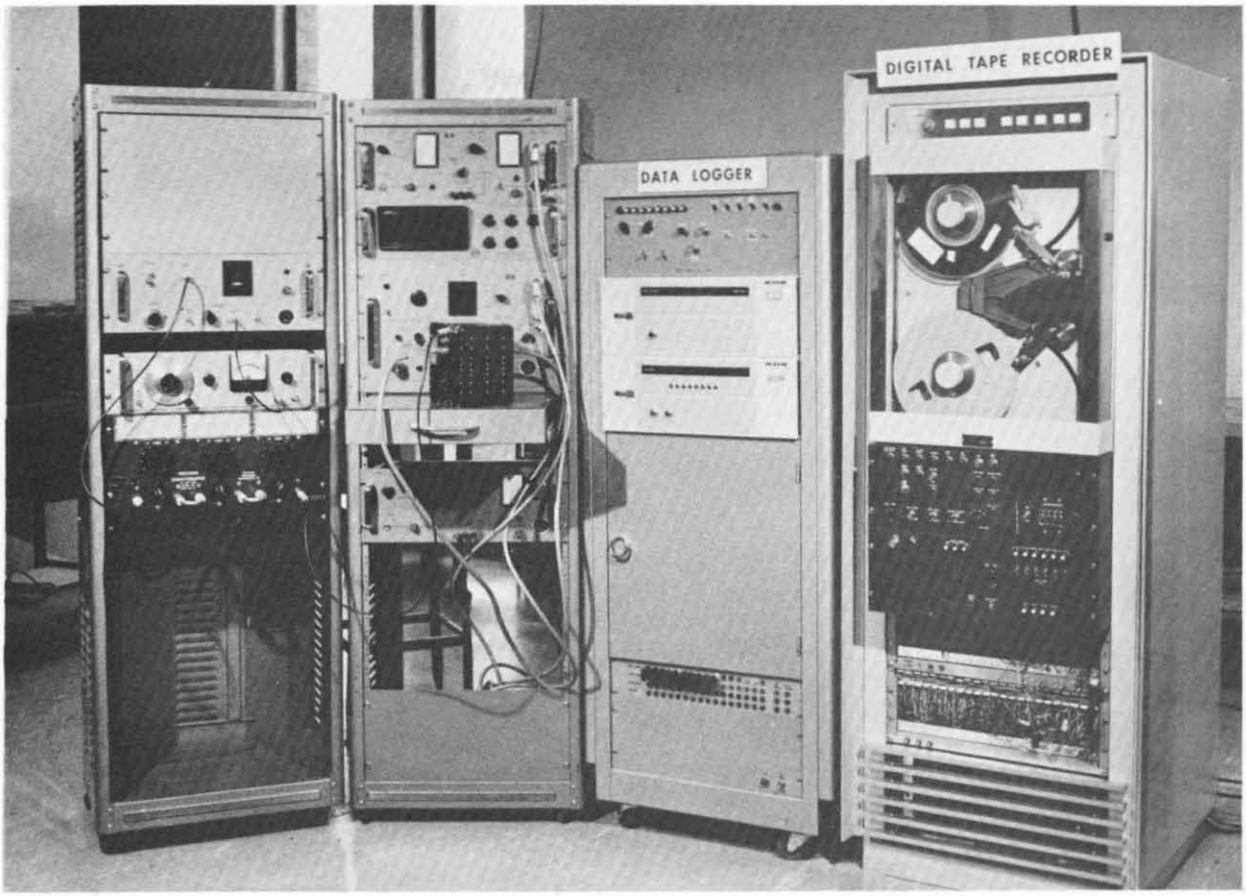

30. Data Logger Facility

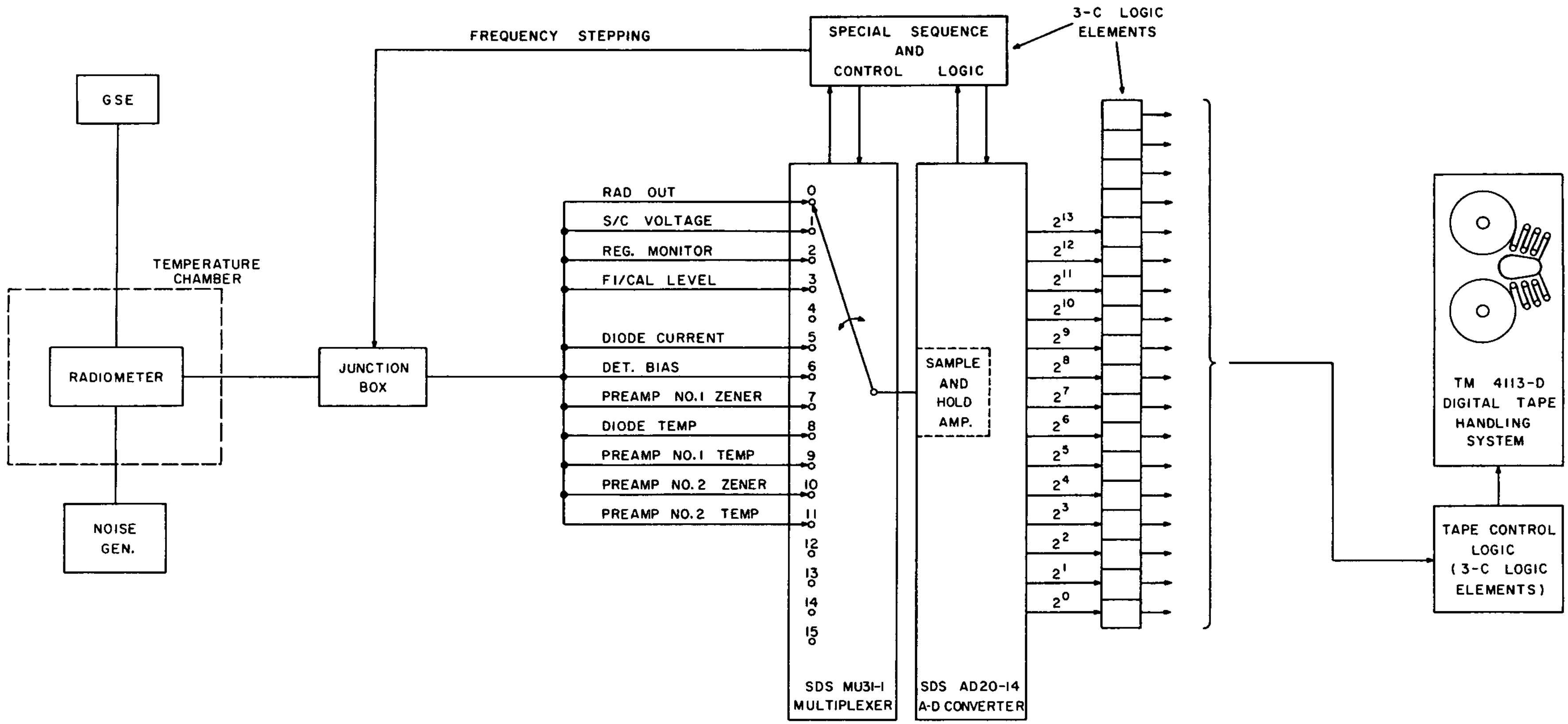

31. Calibration Setup Block Diagram

IMP-I CALIBRATION DATA

28 APRIL 1970 IMP-I 1-01 AND 2-01 FLIGHT CALIBRATION

TEMPERATURE = 0.0 DEGREES C. PREAMP 1

INPUT TAPE NO. UM/RAO 4182

FILE NO. = 1

CALIBRATION VOLTAGES

.253900E 01 -.254400E 01 .508300E 01

GAIN, CHANNELS 0-11, N X 10 .P. -4 = GAIN

.998879E 04 .999823E 04 .100016E 05 .100000E 05 .999607E 04 .998544E 04 .100041E 05 .997895E 04
.991934E 04 .100303E 05 .100315E 05 .999902E 04

OFFSET, CHANNELS 0-11, N X 10 .P. -1 = MILLIVOLTS

.744720E 02 .874956E 02 .530039E 02 .101000E 03 -.870098E 02 -.870364E 02 -.274897E 02 -.505526E 02
-.156202E 03 .129076E 03 .108079E 03 .754975E 02

	FREQ (KHZ)	REC	RAD OTPT	SPPLY VOLT	REG MON	FID/ CALID	DETR BIAS	DIODE CURR	DIODE TEMP	PAMP1 ZENER	PAMP2 ZENER	PAMP1 TEMP	PAMP2 TEMP
INT CAL 1	50	1	3.2183	28.1230	2.2838	4.6858	4.6988	2.5082	3.6886	3.6848	3.7012	2.9169	2.8435
	80	2	3.2784	28.1295	2.2848	4.6874	4.7065	2.5093	3.6902	3.6852	3.7018	2.9182	2.8437
	130	3	3.2965	28.1491	2.2848	4.6868	4.7076	2.5083	3.6893	3.6851	3.7036	2.9186	2.8437
	230	4	3.3370	28.1328	2.2850	4.6864	4.7098	2.5080	3.6891	3.6850	3.7026	2.9184	2.8435
	350	5	3.3064	28.1507	2.2852	4.6865	4.7109	2.5084	3.6892	3.6855	3.7029	2.9184	2.8446
	600	6	3.2946	28.1816	2.2848	4.6870	4.7054	2.5084	3.6895	3.6855	3.7025	2.9183	2.8435
	900	7	3.2798	28.1653	2.2842	4.6849	4.7054	2.5061	3.6882	3.6844	3.7022	2.9174	2.8432
	3530	8	2.5967	28.1426	2.2835	4.6843	4.6856	2.5057	3.6872	3.6836	3.7005	2.9156	2.8416
INT CAL 2	50	9	2.0755	28.1621	2.2831	1.0086	4.6988	2.5087	3.6891	3.6842	3.7020	2.9169	2.8432
	80	10	2.1674	28.1849	2.2839	1.0094	4.7043	2.5084	3.6898	3.6848	3.7032	2.9169	2.8433
	130	11	2.1678	28.2044	2.2836	1.0092	4.6988	2.5079	3.6884	3.6841	3.7022	2.9163	2.8435
	230	12	2.1835	28.1995	2.2828	1.0079	4.6911	2.5076	3.6882	3.6835	3.7002	2.9153	2.8418
	350	13	2.1724	28.2614	2.2842	1.0092	4.6922	2.5073	3.6887	3.6843	3.7020	2.9155	2.8442
	600	14	2.1436	28.1523	2.2841	1.0095	4.7054	2.5075	3.6895	3.6850	3.7024	2.9177	2.8437
	900	15	2.0858	28.1409	2.2843	1.0098	4.7131	2.5075	3.6895	3.6846	3.7027	2.9172	2.8435
	3530	16	1.5500	28.1491	2.2839	1.0087	4.6955	2.5071	3.6884	3.6841	3.7005	2.9158	2.8425
INT CAL 3	50	17	1.0783	28.1735	2.2835	.4199	4.6966	2.5086	3.6891	3.6841	3.7017	2.9160	2.8423
	80	18	1.2617	28.0677	2.2812	.4184	4.6735	2.5052	3.6870	3.6819	3.6984	2.9137	2.8392
	130	19	1.1712	28.1230	2.2842	.4211	4.6999	2.5084	3.6896	3.6842	3.7015	2.9181	2.8432
	230	20	1.0540	28.1458	2.2832	.4201	4.6966	2.5076	3.6893	3.6838	3.7010	2.9155	2.8416
	350	21	.9793	28.1556	2.2825	.4196	4.6911	2.5059	3.6875	3.6829	3.7003	2.9149	2.8406
	600	22	.9694	28.1719	2.2831	.4204	4.6933	2.5058	3.6880	3.6834	3.6998	2.9148	2.8400
	900	23	.9938	28.1702	2.2839	.4210	4.6999	2.5069	3.6891	3.6843	3.7009	2.9163	2.8423
	3530	24	.7014	28.1719	2.2828	.4196	4.6889	2.5062	3.6882	3.6831	3.7003	2.9155	2.8406
INT CAL 4	50	25	.5813	28.2484	2.2816	.4202	4.6911	2.5064	3.6886	3.6831	3.6995	2.9156	2.8404
	80	26	.7204	28.2435	2.2810	.4196	4.6856	2.5063	3.6887	3.6824	3.6983	2.9132	2.8392
	130	27	.4610	28.2744	2.2825	.4206	4.6988	2.5080	3.6898	3.6837	3.7005	2.9156	2.8418
	230	28	.2907	28.2533	2.2815	.4201	4.6900	2.5059	3.6884	3.6824	3.6989	2.9139	2.8399
	350	29	.5134	28.2272	2.2818	.4204	4.6889	2.5058	3.6882	3.6823	3.6993	2.9139	2.8395
	600	30	.2693	28.2158	2.2808	.4186	4.6735	2.5045	3.6870	3.6810	3.6974	2.9123	2.8376
	900	31	.1537	28.2191	2.2806	.4186	4.6746	2.5040	3.6871	3.6811	3.6972	2.9128	2.8376
	3530	32	.2313	28.2077	2.2820	.4201	4.6823	2.5045	3.6877	3.6820	3.6989	2.9146	2.8390
8O3B/NN	50	33	.5845	28.0514	2.2782	1.5358	4.6933	2.5077	3.6926	3.6816	3.6970	3.8135	3.6825

32. Calibration Digital Printout

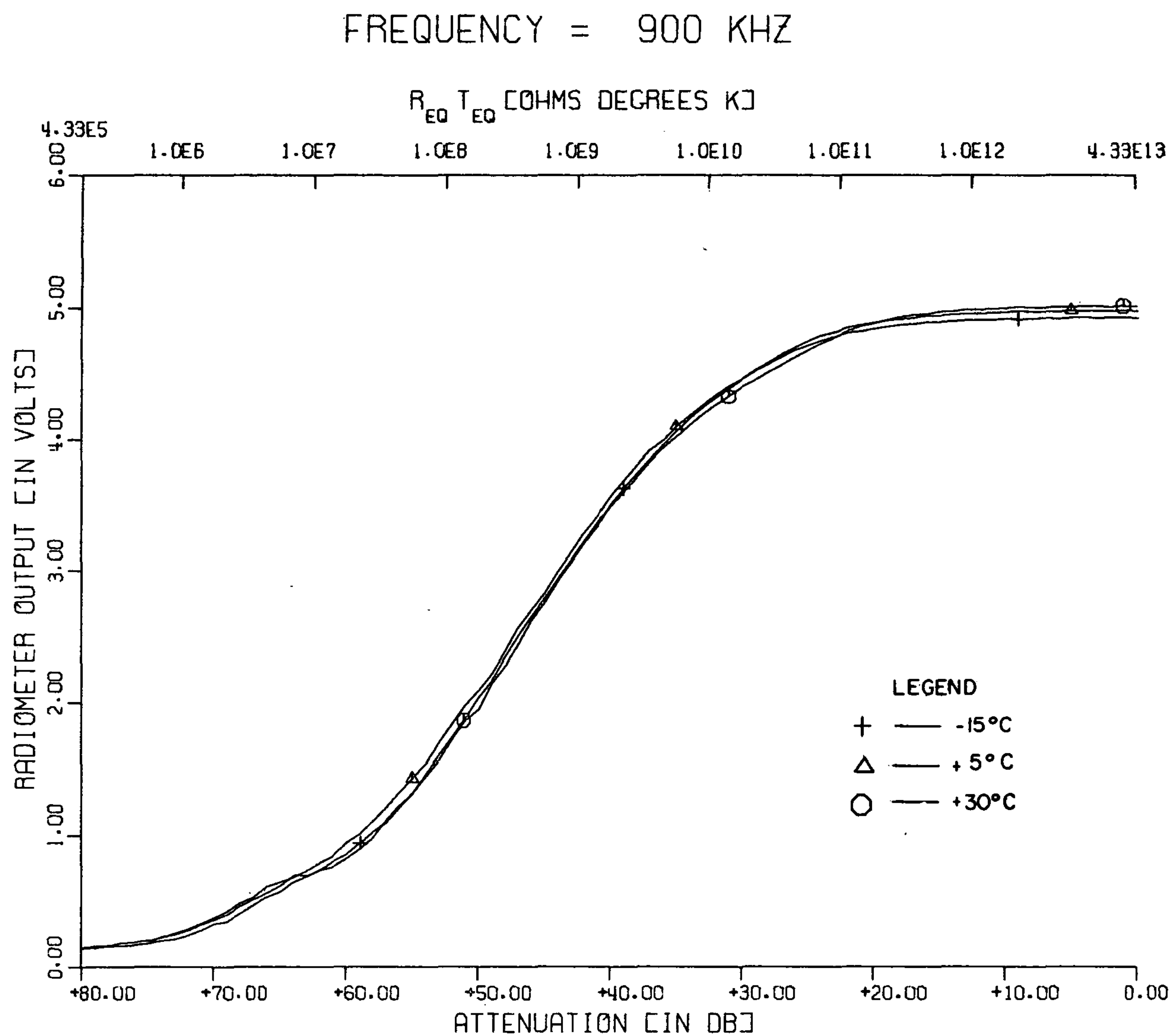

33. **Calibration Calcomp Plot**